Journal of Ethnopharmacology 360 (2026) 121223

Contents lists available at ScienceDirect

Journal of Ethnopharmacology

journal homepage: www.elsevier.com/locate/jethpharm

Catha edulis and Datura stramonium mitigate oxidative stress, mitochondrial dysfunction, and cell death in an SH-SY5Y model of Parkinson's disease

T. Mogale [a], A.D. de Beer [a], W.J. Rudolph [b], V. Steenkamp [a,*]

[a] Department of Pharmacology, Faculty of Health Sciences, University of Pretoria, Pretoria, South Africa
[b] BioDiscovery Centre, Department of Chemistry, Faculty of Natural and Agricultural Sciences, University of Pretoria, Pretoria, South Africa

ARTICLE INFO

Keywords:
Catha edulis
Cytoprotection
Datura stramonium
Oxidative stress
Parkinson's disease

ABSTRACT

Introduction: Parkinson's disease (PD), the second most common neurological disorder, is often managed with medications targeting specific symptoms. Complementing conventional therapies, medicinal plants are frequently used for neurological disorders, including PD. This study evaluated the effects of crude extracts and fractions of *Catha edulis* (Vahl) Forssk. ex Endl. and *Datura stramonium* L.—psychoactive plants—on PD-related mechanisms using SH-SY5Y human neuroblastoma cells.

Method: Crude extracts of *C. edulis* (leaves) and *D. stramonium* (leaf/root mixture) were prepared using dichloromethane/methanol (50/50). Fractionation was performed via C8 solid-phase extraction. Cytotoxicity and cytoprotective effects of the crude extracts and fractions against 6-hydroxydopamine-induced cytotoxicity were assessed using the sulforhodamine B assay. Mechanistic studies included reactive oxygen species (ROS) generation, mitochondrial integrity, and apoptosis assays. *In silico* analysis was used to assess the binding of biomarkers to dopamine receptors.

Results: Both plant extracts exhibited minimal cytotoxicity. Crude extracts and fractions (F1–F7) displayed cytoprotective effects (5.8–34.28 %). The highest ROS reduction was observed for F1 of *C. edulis* (1.72-fold) and F2 of *D. stramonium* (1.33-fold). Both extracts reduced caspase 3/7 activation and maintained mitochondrial integrity. Atropine and scopolamine showed cytoprotection with IC_{50} values of 49.48 μM and 48.26 μM, respectively. *In silico* analysis indicated strong binding affinities of norephedrine and noradrenaline to dopamine D1 and D2 receptors.

Conclusion: Both plant extracts preserved cell viability, reduced ROS levels, and maintained mitochondrial integrity, highlighting their potential as therapeutic agents for PD.

1. Introduction

Parkinson's disease (PD) is the second most common neurological disorder globally, affecting 1 % of people older than 60 (Ou et al., 2021). Over the past 25 years, the global prevalence of PD has doubled. Parkinson's disease symptoms include tremors, balance difficulties, bradykinesia, and stiffness (Bloem et al., 2021). These motor symptoms are connected to the gradual degeneration of dopaminergic neurons in the substantia nigra pars compacta (SNpc), leading to dopamine deficiency in the striatum, a deep brain region involved in voluntary movement (Ramesh and Arachchige, 2023). This dysfunction of the basal ganglia is the primary cause of movement disorders and impaired speech (Sumarac et al., 2024).

Parkinson's disease is also associated with non-motor symptoms,

Abbreviations: 6-OHDA, 6-hydroxydopamine; ACN, Acetonitrile; ATP, Adenosine triphosphate; C I, Complex I; CNS, Central nervous system; Cyt *c*, Cytochrome *c*; DA, Dopamine; DCM, Dichloromethane; DMEM, Dulbecco's modified Eagle's medium; DMSO, Dimethyl sulfoxide; DNA, Deoxyribonucleic acid; ETC, Electron transport chain; EtOAc, Ethyl acetate; FCS, Foetal calf serum; H_2DCFDA, 2′,7′-dichlorodihydrofluorescein diacetate; LC-MS, Liquid chromatography mass spectrometry; MAO, Monoamine oxidase; MeOH, Methanol; MLKL, Mixed lineage kinase domain-like protein; MTBE, Methyl tert-butyl ether; MTT, 3-(4,5-dimethylthiazol-2-yl)-2,5-diphenyl tetrazolium bromide; OS, Oxidative stress; PD, Parkinson's disease; RIPJ 1 and 3, Receptor-interacting protein kinases; ROS, Reactive oxygen species; RFU, Relative fluorescence unit; SEM, Standard error of the mean; SNpc, Substantia nigra pars compacta; SRB, Sulforhodamine B; TCA, Trichloroacetic acid; TRIS, Tris aminomethane; UPLC-UV-QTOF/MS, Ultra-performance liquid chromatography-ultraviolet-quadrupole time-of-flight mass spectrometry.

This article is part of a special issue entitled: ISE-APSS 2024 congress published in Journal of Ethnopharmacology.

* Corresponding author.
E-mail address: vanessa.steenkamp@up.ac.za (V. Steenkamp).

https://doi.org/10.1016/j.jep.2026.121223
Received 3 February 2025; Received in revised form 12 December 2025; Accepted 14 January 2026
Available online 16 January 2026

such as constipation, sensory impairment, insomnia, and neuropsychiatric symptoms (Radad et al., 2023). Motor symptoms remain the primary clinical diagnostic criterion for PD. These symptoms are the result of imbalances in the body. One of these being oxidative stress (OS).

Oxidative stress arises from excessive reactive oxygen species (ROS) production or impaired antioxidant defences (Afzal et al., 2023). In the central nervous system (CNS), microglia and mitochondrial complexes I and III are the primary ROS source (Afzal et al., 2023). A ROS imbalance can cause neuronal damage and cell death (Afsheen et al., 2022). Oxidative stress is central to PD pathophysiology, driven by factors such as genetic mutations, mitochondrial dysfunction, dopamine (DA) autoxidation, iron accumulation, and neuroinflammation, leading to excessive ROS production (Dorszewska et al., 2021). Dopaminergic neurons in the substantia nigra (SN) are particularly vulnerable due to their high oxygen demand and limited antioxidant enzymes (Afzal et al., 2023). In PD, DA metabolism by monoamine oxidases (MAO) and autoxidation in the cytoplasm generates ROS, further exacerbating OS and contributing to neurodegeneration and DA deficiency, which underlie movement disorders in PD (Dorszewska et al., 2021).

Mitochondria are essential for various biological functions, including adenosine triphosphate (ATP) production, calcium homeostasis, lipid synthesis, and apoptosis regulation, with neurons relying heavily on mitochondria due to their high energy demands (Zhou, 2020). The mitochondrial electron transport chain (ETC) generates ATP while producing ROS (Moon and Paek, 2015; Zuo and Motherwell, 2013). Dysfunctions in mitochondrial complexes, particularly complex I (C I), due to genetic mutations (e.g., α-synuclein, LRRK2, parkin, and PINK1) or toxin exposure, disrupt ATP synthesis, calcium homeostasis, and mitophagy, leading to OS and neurodegeneration in PD (Dong-Chen et al., 2023). Antioxidants, both natural (e.g., phenols, flavonoids) and synthetic (e.g., CoQ_{10}), show promise in counteracting OS and preserving mitochondrial function, with clinical and preclinical studies highlighting their potential to protect dopaminergic neurons and slow PD progression (Jiang et al., 2020).

Neuronal death occurs naturally during cell proliferation and in response to pathological conditions such as injury, infection, or genetic abnormalities, primarily via apoptosis and necrosis (Erekat, 2018). Apoptosis, a regulated energy-dependent process, is characterised by cell shrinkage, deoxyribonucleic acid (DNA) fragmentation, and the formation of apoptotic bodies, which are phagocytosed without triggering inflammation (Erekat, 2018). It proceeds via extrinsic (death receptor-mediated) or intrinsic (mitochondrial stress-induced) pathways, both involving caspases that execute the apoptotic cascade (Mustafa et al., 2024). In contrast, necrosis is an uncontrolled process of cell death, triggered by severe stress, leading to cell lysis, membrane rupture, and inflammatory responses (Hajibabaie et al., 2023; Niemann and Rohrbach, 2016). Necroptosis, a programmed form of necrosis, occurs when apoptotic signals are suppressed, activating receptor-interacting protein kinases (RIPK1 and RIPK3), and mixed lineage kinase domain-like protein (MLKL) to cause cell rupture and inflammation (Dhuriya and Sharma, 2018). In neurodegenerative diseases such as PD, apoptosis, necrosis, and necroptosis contribute to neuronal damage, with elevated inflammatory markers and mitochondrial dysfunction playing significant roles in disease progression (Cui et al., 2021).

Plants have been an essential source of medicinal compounds used for treating human illnesses. Recent advancements have focused on standardising herbal remedies and exploring their pharmacological potential (Wang et al., 2023). *Catha edulis* (Vahl) Forssk. ex Endl., commonly known as khat, is a small evergreen shrub belonging to the Celastraceae family, native to Africa and Yemen (Al-Motarreb et al., 2002). It can grow to the height of 2–3 m with a thin trunk, smooth bark, and a deep conical root system (Lamina, 2010). The young leaves are shiny, oval-gladiate in shape, and reddish-green, turning yellow-green upon maturity. The plant produces small white flowers arranged in axillary cymes and develops capsule fruits containing arillate seeds (Magnavacca et al., 2024). Khat is a psychostimulant known for enhancing mental alertness and treating conditions such as obesity and depression, but carries risks such as dependency and cardiovascular issues (Alfaifi et al., 2017). Its active compounds, cathine, cathinone, and norephedrine, exhibit psychostimulatory effects similar to amphetamines (Ye et al., 2021).

Datura stramonium L. commonly referred to as Jimsonweed or thorn apple, is an annual herb belonging to the Solanaceae family and is native to North America (Mishra, 2018). It typically reaches a height of around 1 m, featuring pale green, upright, branching stems. The leaves are oval-shaped with deeply irregularly toothed margins, dark green on the upper surface and lighter in colour on the underside (Yadav et al., 2021). The plant produces large, trumpet-shaped flowers—most commonly white, though occasionally tinged with pale purple—and forms spiny, egg-shaped capsules that split open when mature to release numerous flat, black seeds (Stafford et al., 2005). It is widely used in Africa for the treatment of respiratory ailments and wounds, contains toxic yet therapeutically valuable alkaloids such as atropine and scopolamine (Bussmann et al., 2020; Mishra, 2018) The latter compounds are competitive muscarinic receptor antagonists which, when administered in controlled doses, are used to manage symptoms of PD, among other conditions (Soni et al., 2012).

Over the years, preclinical models, including cell lines and animal models, have been pivotal in understanding the aetiology and pathogenesis of diseases such as PD (Ke et al., 2021). SH-SY5Y cells, derived from a human neuroblastoma, are widely used in PD research due to their dopaminergic properties, expression of neuronal markers, and ability to model key PD characteristics such as OS, mitochondrial dysfunction, and dopaminergic signalling (Cetin et al., 2022; Falkenburger et al., 2016). Neurotoxins such as 6-hydroxydopamine (6-OHDA) are commonly employed to mimic PD-like pathology, targeting dopaminergic neurons and inducing OS (Cetin et al., 2022). 6-Hydroxydopamine damages neurons by entering via the dopamine transporter, undergoing auto-oxidation, and producing ROS, which in turn cause mitochondrial dysfunction, reduce ATP production, and trigger apoptosis (Tamuli et al., 2025). Although SH-SY5Y cells require differentiation to mimic mature neurons, their undifferentiated state offers a reliable platform for studying cytotoxicity and cytoprotection (Lopez-Suarez et al., 2022).

In silico docking, or molecular docking, is a computational technique that simulates the interaction between ligands and target proteins, estimating binding affinity and indicating ideal orientations within receptor sites (Agu et al., 2023; Lemos et al., 2018). This method is particularly valuable in PD research, as it aids in identifying and refining drugs targeting the DA receptors (D1 and D2), which influence motor function irregularities in PD (Kawahata et al., 2024). By predicting ligand-receptor interactions, *in silico* docking accelerates drug development by prioritising promising candidates for experimental testing while reducing the need for extensive screening (Mathur et al., 2024). It also provides insights into receptor modulation, facilitating the design of targeted therapies to improve PD outcomes (Agu et al., 2023).

The aim of this study was to determine the effects of crude extracts and fractions of *C. edulis* and *D. stramonium*—plants recognized for their psychoactive properties—on specific mechanisms of action involved in PD using the SH-SY5Y human neuroblastoma cell line as model.

2. Materials and methods

2.1. Reagents

Acetone and methanol were procured from Merck (Darmstadt, Germany), while BBL™ FTA haemagglutination buffer (used for phosphate-buffered saline preparation) was purchased from BD Biosciences (France). All other reagents were obtained from Sigma–Aldrich (St. Louis, USA). The solvents used for chromatography analyses were of HPLC grade and of the highest purity.

2.2. Plant extract and pure compound preparation

Catha edulis (Vahl) Forssk. ex Endl. (leaves, PM0001) and *Datura stramonium* L. (leaf/root mixture, P12600) was sourced from the Natural Compound Library of the Department of Chemistry, University of Pretoria. Voucher specimens of the plants were prepared and submitted to herbaria. The specimen of *D. stramonium* (spec. no. PRE0894074-0) was submitted to the South African National Biodiversity Iinstitute (SANBI) Herbarium (Pretoria, South Africa). *C. edulis* was submitted to the H.G. W.J. Schweickerdt Herbarium at the University of Pretoria (spec. no. PRU 121 392).

Plant material was extracted following a method adapted from Invernizzi et al. (2022). Ground plant material (7.0–7.3 g) and 50 mL dichloromethane (DCM): methanol (MeOH), at a ratio of 1:1 was added to sintered glass funnels, which were partially submerged in an ultrasonic bath for 1 h at 25 °C. After the first extraction, the solvent mixture was filtered into round-bottom flasks and stored at room temperature in the dark. The marc was similarly extracted a second time with 100 % MeOH (50 mL). The DCM:MeOH and MeOH extracts were combined in a round bottom flask and dried under reduced pressure using a rotary evaporator. After drying, the extracts were reconstituted in MeOH, transferred into pre-weighed 20 mL glass polytops, and dried at 35 °C for 6 h using a Genevac® EZ-2 Plus Mk III centrifugal evaporator.

After drying, 200–250 mg of the crude extract was transferred into pre-weighed 10 mL plastic tubes for fractionation. The crude extract was reconstituted in a 6:3:1 mixture of MeOH: ethyl acetate (EtOAc): methyl tert-butyl ether (MTBE), the amount which was determined by the automated liquid handler (Hamilton® Microlab® STARLET™ M) and vortex-mixed until solubilised. A sample, containing 5 mg extract, was transferred to a 96 deep-well plate for standardization in the Bio-Discovery Library. The remainder was decanted onto dental cotton wool in 10 mL glass polytop vials and dried under reduced pressure in a centrifugal evaporator. Once dried, the crude extract-saturated cotton wool was inserted into empty 6 cc polypropylene Phenomenex® solid-phase extraction (SPE) cartridges containing a single frit and stored at 4 °C till use.

Fractionation was carried out using a Gilson® GX-241 ASPEC® liquid handler, connected to a Gilson® Verity® 4060 solvent pump, and C8 HyperSep® 2 g/6 mL cartridge (Mianda et al., 2022). The cartridge stationary phase was activated with 100 % MeOH (20 mL), thereafter equilibrated with MeOH: H_2O (5:95, 20 mL). The cotton wool-loaded cartridges were fitted onto C8 HyperSep® cartridges and eluted at a flow rate of 10 mL/min with a washout step to clean the injector between each solvent system. Fractions were labeled with the suffix F1 to F7 to indicate the gradient solvent system used. An aqueous solvent system was used for F1 to F6 with an increasing concentration of MeOH, and F7 consisted of MeOH: acetonitrile (ACN) [1:1, v/v]. After fractions were eluted under positive pressure, each fraction was stored in a barcoded plastic tube. The fractions were then dried under reduced pressure for 14 h using the Genevac® HT-6 Series 3i centrifugal evaporator. Once dry, the tubes were placed into polyurethane bags and stored at 4 °C for future use.

At the time of use, dried samples in the deep-well plates were reconstituted using biological-grade dimethyl sulfoxide (DMSO) to achieve a final concentration of 5000 µg/mL. The reconstituted samples were transferred to FluidX® 1.0 mL EXT Co-Mold Jacket tubes, facilitated by the MicroLab® STARLET™ system. Aliquots (40 µL) were pipetted into a deep-well plate and heat-sealed with an aluminium heat sealer (BIOBASE® PS-2 Semi-automated plate sealer). Plates were stored at −80 °C to ensure no phytochemical degradation occurred. The samples in the FluidX® tubes are stored in a Hamilton® Verso® Q20 -20 °C freezer.

Phytochemical markers (pure compounds), atropine and scopolamine, identified from the literature, were purchased from Sigma–Aldrich (St. Louis, USA). Stock concentrations were prepared in DMSO and diluted to the desired working concentration.

2.3. Ultra-performance liquid chromatography-ultraviolet-mass spectrometry

Dried crude stock extracts and fractions were reconstituted in water: MeOH [1:1, v/v] (ROMIL® SpS-grade Methanol 215). The samples were filtered through 0.22 µm nylon syringe filters (Agela® Technologies), where after the stock solutions were diluted to a concentration of 5000 ppm in 1.5 mL sample vials.

The samples were analysed using ultra-performance liquid chromatography-ultraviolet spectroscopy-quadrupole time-of-flight mass spectrometry (UPLC-UV-QTOF/MS) in both the positive and negative ionisation modes as described by (Invernizzi et al., 2022). For elution of the samples, a generic methanol/water (+0.1 % v/v formic acid)-based solvent system was used at a flow rate of 0.3 mL/min. Separation of the sample constituents was achieved on an XBridge UPLC® C18 BEH (2.1 × 150 mm, 1.7 µm) column (Waters ® Inc., Milford, MA, USA).

Eluting constituents were first detected by an in-line Acquity eλ photodiode array (PDA) detector, set over the wavelength range 220–700 nm. Thereafter, high resolution mass spectrometry data was acquired on the ions generated by electrospray ionisation on a Waters Xevo G2 QTof mass analyser. Leucine enkephalin (m/z ESI+ = 556.2771; m/z ESI- = 554.2615) was used as an internal accurate mass reference and introduced in-source every 20 s.

2.4. Cellular experiments

2.4.1. Cell culture and maintenance

The SH-SY5Y neuroblastoma cells (ATCC CRL-2266) were cultured in T_{25} cm^2 flasks with a 1:1 mixture of Ham's F12 medium and Dulbecco's modified Eagle's medium (DMEM). The medium was supplemented with 10 % foetal calf serum (FCS), and 1 % penicillin-streptomycin. The cells were incubated (HF 212 UV incubator) at 37 °C in a 5 % CO_2 humidified atmosphere. The medium was changed twice a week, and cells were split when a ~80 % confluency was reached. Confluent cells were washed with 1 mL medium free of FCS, and enzymatically detached by adding 3 mL trypsin-like enzymes solution for 4 min. Cells were harvested using centrifugation (5 min, 200 *g*), and the pellet was re-suspended in 1 mL culture medium. Cells were counted using the trypan blue exclusion assay (0.1 % w/v) and re-suspended to 1 x 10^4 cells/mL for the 96-well plate assays.

2.4.2. Cytotoxicity determination

The sulforhodamine B (SRB) assay as described by Vichai and Kirtikara (2006), with adjustment to the volumes, was used to determine cytotoxicity. Cells were seeded at a density of 10 000 cells per well (100 µL) in a 96-well plate and incubated overnight for cellular attachment. Cells were exposed to either 100 µL medium (negative control), 0.5 % DMSO (vehicle control), 1 % saponin (positive control), 6-OHDA (5–150 µM, in-well concentrations), crude extracts (1, 3.1, and 10 µg/mL, in-well concentrations), F1 to F7 (1, 3.1, and 10 µg/mL, in-well concentrations) or pure compounds (5–200 µM in-well concentrations) in FCS-free medium for 48 h. Blanks consisting of 5 % FCS-supplemented medium were used as background noise control.

Following exposure, the cells were fixed by adding 50 µL of a 50 % (v/v) trichloroacetic acid (TCA) solution to each well. The plates were incubated at 4 °C overnight, where after the plates were washed using running tap water. This was followed by drying the plates in an oven at 40 °C for approximately 1 h. Thereafter, 100 µL of a 0.057 % (w/v) SRB stain in 1 % acetic acid was added to all wells, and the plates incubated in the dark for 30 min at 25 °C. Excess SRB stain was removed by washing the cells with 150 µL acetic acid, and this wash step was repeated until all unbound stain was removed. Thereafter, the plate was dried in the oven for approximately 30 min. The bound dye was solubilised by adding 200 µL of tris aminomethane (TRIS) buffer (10 mM; pH 10.5) to the wells, after which the plate was covered with aluminium foil

and placed on an orbital plate shaker for 1 h. The plate was then placed in a plate reader (Synergy 2 HTX Multi-Mode plate reader), and the absorbance was read at 510 nm with a reference wavelength of 630 nm. Cell density was calculated using the following equation:

$$Cell\ density\ (\%) = \frac{Average\ absorbance(test\ compound)}{Average\ absorbance\ (NC)}\ x\ 100$$

2.4.3. Determination of cytoprotection

6-Hydroxydopamine (72.83 μM) was used to induce PD-like neurotoxicity. Cells were seeded as described previously and exposed to 50 μL of 6-OHDA for 2 h. Thereafter cells were exposed to 50 μL either 1 % saponin (positive control), crude extracts or fractions (F1 to F7) (at in-well concentrations of 1, 3.1, and 10 μg/mL) or pure compounds; atropine (in-well concentrations 49.48 μM) or scopolamine (in-well concentrations 48.26 μM) for 48 h. The SRB assay was used to assess cytoprotective ability, which was measured by the difference in cell density of the treated wells compared to the 6-OHDA control.

Cell morphology was captured using phase contrast microscopy (Zeiss Axiovert CFL40 microscope, Carl Zeiss AG, Oberkochem, Germany).

2.5. Determination of intracellular reactive oxygen species

The enzymatic cleavage of 2′,7′-dichlorodihydrofluorescein diacetate (H_2DCFDA) to the highly fluorescent dichlorofluorescein, as described by Brubacher and Bols (2001), was used to determine intracellular ROS concentrations. Cells were seeded and exposed as described previously. Potassium persulfate (1 mM in-well concentration) was used as the positive control. After 48 h treatment, the medium was replaced with 100 μL H_2DCFDA (10 μM in PBS) followed by 2 h incubation at 37°C. The fluorescence intensity was measured at an excitation wavelength of 480 nm and an emission wavelength of 590 nm. The ROS concentration was determined using the formula:

$$Intracellular\ ROS\ concentration\ (\ \%\ \ of\ negative\ control) = \frac{FI_s}{FIc} \times 100$$

With FI_s being the normalised fluorescence intensity of the blank-adjusted sample and FI_c being the normalised average of the blank-adjusted negative control.

The 3.1 μg/mL concentration was used in all subsequent mechanistic assays, as it was the concentration which showed most consistent results.

2.6. Determination of apoptosis

The Ac-DEVD-AMC cleavage assay as described by Cordier and Steenkamp (2018) was used to determine caspase-3/7 activity. Cells were seeded and exposed as described earlier, for 48 h. Cisplatin (29.85 μM in-well concentration) served as the positive control. After the 48 h incubation period, the medium was replaced with 25 μL of cold lysis buffer (10 mM HEPES, 2 mM CHAPS, 5 mM EDTA, 0.5 mM PMSF, 4.3 mM β-mercaptoethanol) and incubated for 15 min on ice. Thereafter, 100 μL of substrate buffer (10 μM Ac-DEVD-AMC, 10 mM HEPES, 5 mM EDTA, 0.5 mM PMSF, 4.3 mM β-mercaptoethanol) was added, and the plate incubated for 4 h at 37°C. The fluorescent intensity (FI) was measured at an excitation of 355 nm and emission of 460 nm using the Synergy II plate reader, which was adjusted by subtracting the blank value with normalisation relative to caspase 3/7 activity and cell density relative to the negative control as per the equation:

$$Caspase-3/7\ activity\ (Fold-change\ relative\ to\ negative\ control) = \frac{FI\ sample}{FI\ of\ average\ negative\ control}$$

2.7. Determination of mitochondrial integrity

Mitochondrial integrity was assessed using the cytopainter mitochondrial staining kit (ab112145, Abcam, UK). All procedures were performed according to the manufacturer's instructions. Cells were seeded and exposed as described earlier. Potassium persulfate was used as positive control (1 mM in-well concentration). After exposure, the media was removed and replaced with 100 μL of a 0.3 times dilution of the cytopainter red (6 μL of 500x dye to a total of 10 mL FCS-free media). The plate was then incubated for 30 min in a humidified incubator at 37°C. After incubation, the dye was replaced with 100 μL FCS-free media. Fluorescence was read using a plate reader (FLUOstar optima) set at an excitation and emission wavelength of 544 nm and 620 nm, respectively. The relative fluorescence unit (RFU) was compared to the negative control and normalised by the cell density. Results are expressed as a ratio of the mitochondria to cell density compared to the negative control.

2.8. In silico docking

Molecular docking simulations were conducted following the protocol established by Friesner et al. (2004), enabling evaluation of ligand–receptor interactions at the molecular level.

2.8.1. Protein preparation

Protein preparation was performed using the Protein Preparation Wizard in Maestro. During this process, water molecules were removed, bond orders were assigned, and hydrogen atoms were added to the chemical structures of the phytochemical markers detected in *C. edulis* and *D. stramonium*. Additionally, bonds to metals were deleted, and formal charges on the metals and neighbouring atoms were adjusted within a specified range. Thereafter the protonation state for the residues in the chemical structures were adjusted to reflect physiological conditions and minimise potential errors in structures. The chemical structure was then refined with a restrained minimisation to reduce steric clashes and optimise geometry while maintaining the overall conformation. Potential binding sites were identified using a grid-based cavity prediction algorithm, with the OPLS-2005 force field applied for energy minimisation.

2.8.2. Ligand preparation

Ligand preparation was initiated by constructing the 2D structure of each compound detected in *C. edulis* and *D. stramonium* using SMILES conversion on Chem Draw Ultra 10.0. The 2D structures were then converted to a 3D structure using the same software. The software's SMILES conversion feature ensured the correct initial molecular structure, including proper chirality. The aim was to generate a low-energy 3D structure for each input, which accurately reflected the proposed molecular geometry.

Further ligand refinement was conducted using the LigPrep module in Maestro. In this step, chirality was preserved from the 3D structure, and the original ionisation states of the ligands were maintained. Tautomers were generated during this process, replacing any existing conformers to ensure that different possible forms of the ligand were considered. The conformational space was explored using the Monte Carlo method, a robust algorithm for finding the global minimum by testing a wide range of possible conformations. The search involved exploring all rotatable single bonds to account for the flexibility of the ligand. This process identified the global energy minimum multiple times, confirming the most stable ligand conformations.

Finally, the OPLS_2005 force field was applied during the energy minimisation step, ensuring accurate structural refinement based on the least square minimisation approach. This methodology ensured that the ligand was prepared with the lowest energy, best conformer, and appropriate molecular properties for subsequent molecular docking or

simulation studies.

2.8.3. Active site determination

Using the Glide docking model, grids were generated to evaluate the binding interactions between the ligand and the protein's active sites. These grids were created using the Receptor Grid Generation module in Glide, following standard procedures to define the receptor's active site. The generation of grids involves mapping the electrostatic and geometric properties of the receptor to provide an accurate docking environment. The grid defined the shape and electrostatics of the receptor, allowing for the precise placement of ligands within the protein's active site. Additionally, constraints were incorporated into the grid files, ensuring that certain critical interactions (such as hydrogen bonds with specific residues) were included during docking. Multiple fields were used to represent the receptor's properties, progressively enhancing the accuracy of ligand scoring. This included factors like steric and electrostatic complementarity, which are essential for determining the favourable binding poses of the ligand. This comprehensive approach allowed the Glide model to predict optimal ligand-receptor interactions, providing insights into binding strength and mode, and supporting drug discovery by identifying potential therapeutic targets.

2.8.4. Molecular docking

A ligand molecule was selected so that it could be excluded from the grid generation with the van der Waals radius scaling set to 1.00. The ligand was docked using the docking functionality in extra precision (XP) mode. The most feasible orientation of the ligands in the binding pocket was predicted, and the strength of the interaction in that orientation was quantified from a scoring function.

2.8.5. Targets for docking

Molecular docking was employed to examine the interactions between phytochemical markers identified in *C. edulis* and *D. stramonium* with both dopamine receptors (D1 and D2).

2.9. Statistical analysis

Raw data was captured using Microsoft Excel (Microsoft Office Suite) and statistical analyses were performed using GraphPad Prism 8.0.2. At least three biological and technical repeats were performed ($n \geq 9$). All data was expressed as the mean ± standard error of the mean (SEM). Changes in protein content was calculated using the Kruskal-Wallis analysis of variance test with Dunn's multiple comparison post-test. For cytotoxicity studies, the logarithm of the concentration of the crude extracts/fractions/isolated compounds was plotted against the response (reduction in cell density – compared to the positive control (6-OHDA). Outliers were identified and removed using GraphPad Robust regression and the outlier removal (ROUT) method. The indicator of significance was $p \leq 0.05$.

3. Results and discussion

3.1. Phytochemistry

The phytochemical profiles of *C. edulis* (Vahl) Forssk. ex Endl. and *Datura stramonium* L. encompass a diverse array of secondary metabolites, including alkaloids, flavonoids, and phenolic compounds, which underpin their pharmacological and therapeutic properties (Getasetegn, 2016; Sharma et al., 2021). *C. edulis* is characterised by its phenylpropylamino alkaloids, including cathine and cathinone, which act as CNS stimulants (Ye et al., 2021). *Datura stramonium* is distinguished by its tropane alkaloids, including atropine, hyoscyamine, and scopolamine, which exhibit potent anticholinergic activity and have been extensively studied for their neuropharmacological importance (Soni et al., 2012).

In the chromatogram of *C. edulis* (Fig. 1), peaks A and B likely correspond to closely eluting molecules, tentatively identified as cathine and/or norephedrine (Table 1). Compound A was detected only in the crude extract and fraction 2 (F2), whereas compound B was present in the crude extract and all fractions, with pseudo-molecular ions at m/z = 152.1084. Similarly, Dhabbah et al. (2018) detected peaks corresponding to cathine in *C. edulis* leaves at m/z = 152.11 using direct analysis in real time (DART) TOF-MS. Supporting these results, Field (2001) identified a peak for cathine at m/z = 151 in methanolic extracts of *C. edulis* using GC/MS, thereby corroborating the earlier findings.

Only cathine and its isomer, norephedrine, were provisionally identified from among the known chemotaxonomic markers of *C. edulis*. Both compounds are metabolites of S-(−)-cathinone, and their relative abundances are influenced by environmental conditions at the time of harvest (Wabe, 2011). Furthermore, this compound is unstable and prone to oxidation during drying or processing of the plant material (Wabe, 2011). Despite sharing the same chemical structure and accurate mass, cathine and norephedrine are stereoisomers, differ subtly in their 3D structures (Ali et al., 2011). These structural differences are reflected in their closely related retention times and accurate masses, as shown in Table 1.

The chemotaxonomic markers: hyoscyamine, noradrenaline, and atropine were identified in *D. stramonium* (Table 1). However, as seen in Fig. 2, the peak for atropine (C) was not easily distinguishable due to co-elution with hyoscyamine. The co-elution is likely a result of their nearly identical molecular weights and similar chemical structures as stereoisomers, making their chromatographic separation challenging (Antoine Lanfranchi et al., 2010).

In the crude extract, all three compounds appeared as overlapping

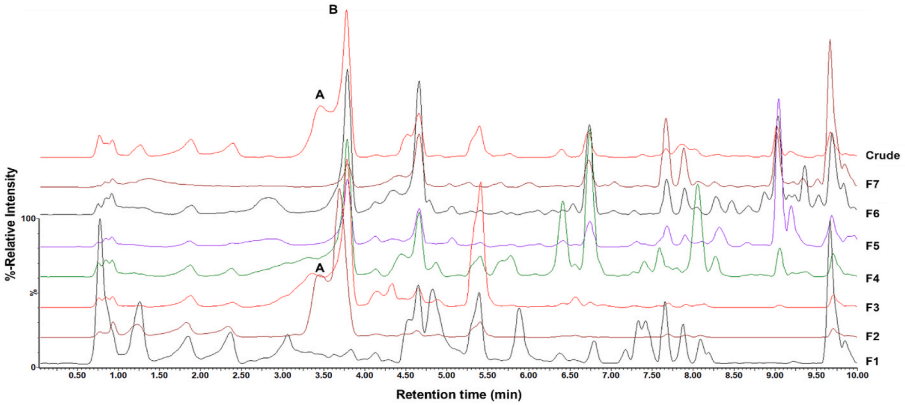

Fig. 1. Chromatograms of *Catha edulis* crude extract and fractions (F) 1–7 analysed in the positive electrospray ionisation mode. Peaks: A and B: cathine or norephedrine.

Table 1
Phytochemical markers detected in the crude extract and fractions of *Catha edulis* and *Datura stramonium* using ultra-performance liquid chromatography-mass spectrometry.

	Peak retention time (min)	Identified compound	m/z Ion	Molecular Weight (g/mol)	Neutral mass (Da)	Theoretical mass (Da)	Mass difference (ppm)	λ_{max} (nm)
Catha edulis	**A 3.461**	Cathine or Norephedrine	152.1084 $[M+H]^+$	151.21	151.1011	151.0997	9.27	295
	B 3.791	Cathine or Norephedrine	152.1084 $[M+H]^+$	151.21	151.1011	151.0997	9.27	295
Datura stramonium	**A 5.286**	Hyoscyamine	290.1750 $[M+H]^+$	289.375	289.1676	289.1678	−0.735	295
	B 5.491	Noradrenaline	153.0551 $[M + H\text{-}NH_3]^+$	169.18	169.0739	169.0739	−0.215	295
	C 5.437	Atropine	290.1749 $[M+H]^+$	289.369	289.1676	289.1678	−0.479	295

min: minutes, Da: Daltons, ppm: parts per million, nm: nanometer.

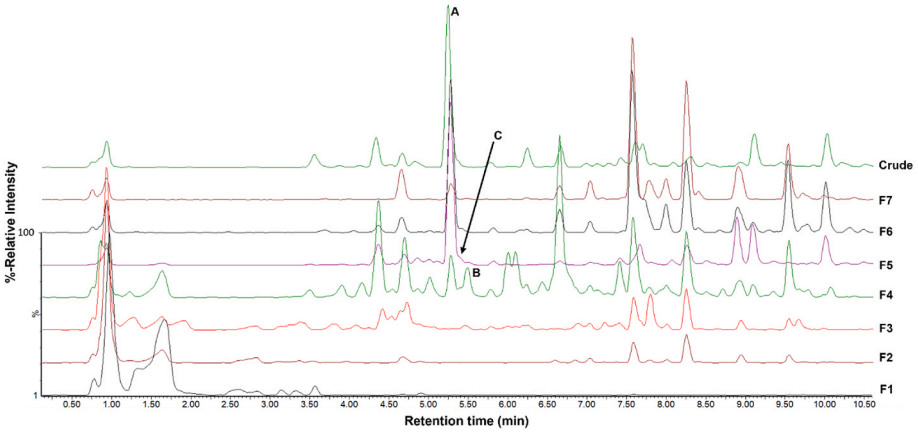

Fig. 2. Chromatograms of *Datura stramonium* crude extract and fractions (F) 1–7 analysed in the positive electrospray ionisation mode Peaks: A: Hyoscyamine, B: Noradrenaline, C: Atropine.

and broad peaks, reflecting the presence of a complex mixture of secondary metabolites. This co-elution resulted in reduced resolution of individual compound peaks. Fractionation, however, improved separation, with the resulting fractions exhibiting distinct intensities and well-defined peak profiles (Fig. 2).

Hyoscyamine and atropine were more prominent in the crude extract, as well as in F5 and F6. This finding is consistent with that of Yadav et al. (2021) who only detected atropine and hyoscyamine using GC-MS analysis. Noradrenaline was most prominent in F4, indicating successful polarity-based separation. The compounds of interest were absent in F1–F3, due to the selectivity of the SPE-fractionation process. Interestingly, scopolamine, one of the chemotaxonomic markers of *D. stramonium*, was not detected in the extract, likely due to its very low concentration. Furthermore, the ultrasonication extraction method method may have contributed to its degradation, as the localised cavitation and rapid temperature increases associated with this technique may degrade unstable compounds like scopolamine (Vassilakis et al., 2004). Miraldi et al. (2001) reported that atropine (0.134 μg/mg) was present at much higher concentrations than scopolamine (0.044 μg/mg) in trichloromethane leaf extracts of *D. stramonium* L. when quantified using GC-MS. In contrast, Jakabová et al. (2012) noted higher scopolamine concentrations (3.94 μg/mg) compared to atropine (0.03 μg/mg) in methanolic flower extracts of *Datura inoxia* Mill. using LC-MS. These differing results indicate that scopolamine concentrations may vary considerably depending on the plant species and the plant part analysed, with lower levels present in the leaves and higher levels in the flowers. Its absence in our extract could be due to its low abundance in the leaves and roots utilised, as well as potential degradation during extraction given its known instability. It is well established that phytochemical content can differ depending on the specific plant part, soil conditions, and the time of year the plant is collected (Jakabová et al., 2012). Additionally, alkaloid concentrations are known to generally vary across different plant tissues, further contributing to the observed differences in scopolamine levels (Jakabová et al., 2012).

Hyoscyamine and atropine, both tropane alkaloids, exhibited similar retention times (Table 1) due to their structural similarities, while noradrenaline, a hydrophilic phenylpropylamino alkaloid, eluted earlier, consistent with its polarity. These results demonstrate the efficiency of the fractionation process in isolating bioactive compounds while highlighting potential challenges in separating structurally similar alkaloids under the chromatographic conditions employed.

3.2. Cytotoxicity of the crude extract and fractions

The crude extract and F1, F2, F4, and F6 of *C. edulis* exhibited minimal albeit concentration-dependent cytotoxicity in the SH-SY5Y cells (Fig. 3A). At lower concentrations (1 μg/mL), the fractions increased cell density by ~10 %, likely due to a hormetic effect, whereas at higher concentrations cytotoxicity was evident. In contrast, F3 and F5 did not induce concentration-dependent cytotoxicity, nor was there a significant reduction in cell viability noted for most of the tested concentrations. However, at 10 μg/mL, the crude extract and F6 significantly reduced cell density by 17.9 % ($p < 0.001$) and 12.34 % ($p < 0.0001$), respectively. Among the tested samples, the *C. edulis* crude extract demonstrated the highest cytotoxicity, significantly ($p < 0.0001$) decreasing cell density by approximately 17.9 % at 10 μg/mL.

The minimal cytotoxicity noted for *C. edulis* is supported by other studies. Synthetic cathinone has been shown to exert a dose-dependent

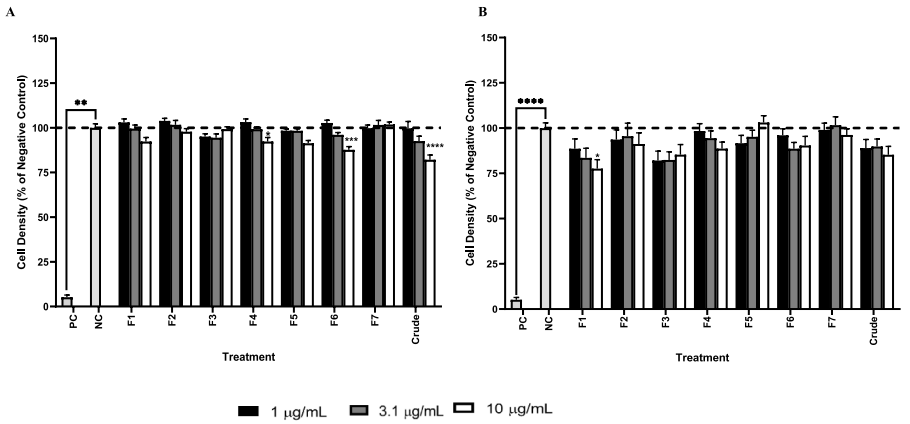

Fig. 3. The cytotoxic effect of *Catha edulis* (A) and *Datura stramonium* (B) crude extract and fractions (F1 - F7) on the SH-SY5Y cells. Values are shown as means ± SEM of three biological and technical repeats (n = 9). Significance was determined relative to the negative control; *p < 0.05, **p < 0.01, ***p < 0.001, ****p < 0.0001. NC: negative control (FCS-free media) and PC: positive control (1 % saponin).

cytotoxic effect in SH-SY5Y cells (Leong et al., 2020). Similarly, Valente et al. (2017) reported dose-dependent cytotoxicity in SH-SY5Y cells, noting that synthetic cathinones such as 3,4-methylenedioxypyrovalerone (MDPV) caused minimal cell death at lower concentrations (0.1 mM) but substantially higher cell death at elevated concentrations (10 mM).

It can thus be deduced that cathinones, including those naturally present in *C. edulis*, are less toxic at lower doses, which corroborates the minimal cytotoxicity observed in this study. Furthermore, *C. edulis* also contains alkaloids, flavonoids, and other phytochemicals, which may contribute to its reduced cytotoxicity. It is possible that these compounds interact in a way that mitigates the potential cytotoxic effects (Getasetegn, 2016).

Fractions 1, 4, and 5 of *D. stramonium* displayed concentration-dependent cytotoxicity in SH-SY5Y cells (Fig. 3B). Fraction 1 reduced cell density by 11.43 %, 16.47 %, and 22.41 % ($p < 0.05$) as concentrations increased from 1, 3.1, to 10 µg/mL, respectively. Fraction 4 reduced cell density by 11.37 % at 10 µg/mL. Fraction 5 reduced cell density by 8.39 % and 4.84 % at lower concentrations (1 and 3.1 µg/mL), while at 10 µg/mL, there was a slight increase in cell density of 3.07 %. The crude extract and F2, F3, F6 and F7 induced minimal cytotoxicity (Fig. 3B).

The minimal cytotoxicity observed for *D. stramonium* extract could be attributed to the concentrations that were tested being below the potential cytotoxic threshold. It has been reported that the methanol extract's IC_{50} was 39.48 µg/mL, suggesting that concentrations below this value are unlikely to cause significant cytotoxicity (Pallavi Sharma et al., 2014). Studies on other Solanaceae plants with similar alkaloid profiles, such as *Datura inoxia* Mill. and *Hyoscyamus niger* L., have demonstrated comparable results. *Datura inoxia* Mill. methanol extract exhibited concentration-dependent cytotoxicity, reducing cell viability to below 50 % at concentrations above 25 µg/mL, with an IC_{50} of 66.53 µg/mL in PC12 cells, while at lower concentrations (3.125–12.5 µg/mL) cell viability was maintained at ≥ 90 % (Vélez-Huerta et al., 2022). Similarly, *H. niger* demonstrated neuroprotective effects in rotenone-induced rat models by restoring the activity of antioxidant enzymes, superoxide dismutase and catalase, and increasing glutathione levels (Sengupta et al., 2011). These findings suggest that *D. stramonium*, like other Solanaceae plants, may exert minimal cytotoxicity at lower concentrations, possibly due to their alkaloid composition and associated antioxidant properties.

3.3. Cytotoxicity of 6-hydroxydopamine

6-Hydroxydopamine exerted a concentration-dependent effect on cell viability, with an IC_{50} of 72.83 µM. No further cytotoxicity was observed at higher concentrations, as the cell density plateaued. This could be ascribed to a saturation effect, where a threshold concentration maximises cell death or the presence of cellular resistance mechanisms that prevent additional cytotoxicity. The results are corroborated by Luo et al. (2022) where the authors reported that treatment with 6-OHDA (75 µM) significantly reduced the viability of SH-SY5Y cells to approximately 60 % after 24 h of treatment using the 3-(4,5-dimethylthiazol-2-yl)-2,5-diphenyl tetrazolium bromide (MTT) assay.

Wei et al. (2015) reported an IC_{50} of 100 µM for 6-OHDA in SH-SY5Y cells following 24 h of treatment, as determined by the MTT assay. Similarly, Pasban-Aliabadi et al. (2013) observed a dose-dependent effect, with an IC_{50} of 150 µM after 24 h of incubation using the same assay. The higher IC_{50} values may be attributed to varying experimental parameters, including the assay used; MTT versus SRB, cell line variability, and incubation times (Ju et al., 2010).

The state of cell differentiation is also of importance, as it leads to the up-regulation of enzymes and transporters such as tyrosine hydroxylase and dopamine transporter. SH-SY5Y cells differentiated using retinoic acid and 1 % foetal bovine serum were found to have increased vulnerability to 6-OHDA-induced cytotoxicity (Lopes et al., 2010; Xie X et al., 2010). Despite these variations, the current results offer valuable insights into the cytotoxic effects of 6-OHDA on SH-SY5Y cells. It was therefore decided to determine the activity of the plant extracts relative to the IC_{50} concentration of 6-OHDA (72.83 µM).

3.4. Cytoprotection of the crude extract and fractions

In the PD model, 6-OHDA acts as an OS inducer, playing a crucial role in the pathogenesis of PD. It has been demonstrated that 6-OHDA-induced cytotoxicity in SH-SY5Y cells is dependent on both the concentration and exposure time. A reduction in cell viability of 35 % was noted after treatment with 100 µM 6-OHDA for 24 h (Silva et al., 2018). In the present study, treatment with 6-OHDA alone resulted in a significant ($p < 0.0001$) decrease in cell density by ~ 81.38 % (Fig. 4).

Dose-dependent cytoprotection was observed when cells were treated with *C. edulis* F1, F2, and F6 (Fig. 4A). Concerning F1, cell density increased significantly for the three concentrations tested, compared to the control. Fraction 2 increased cell density by 11.85 %, 5.12 % and 0.44 % at concentrations of 1, 3.1, and 10 µg/mL, respectively. Fraction 6 significantly increased cell density at all three concentrations tested, with 1 and 3.1 µg/mL showing significance at $p < 0.01$, and 10 µg/mL at $p < 0.05$, compared to the control. Fraction 3 showed similar increases in cell density for both the 1 and 10 µg/mL concentrations of 9.7 % ($p < 0.001$). Of all the fractions, F1 displayed the highest cytoprotection.

Although *C. edulis* extract exhibited cytoprotection, the level was

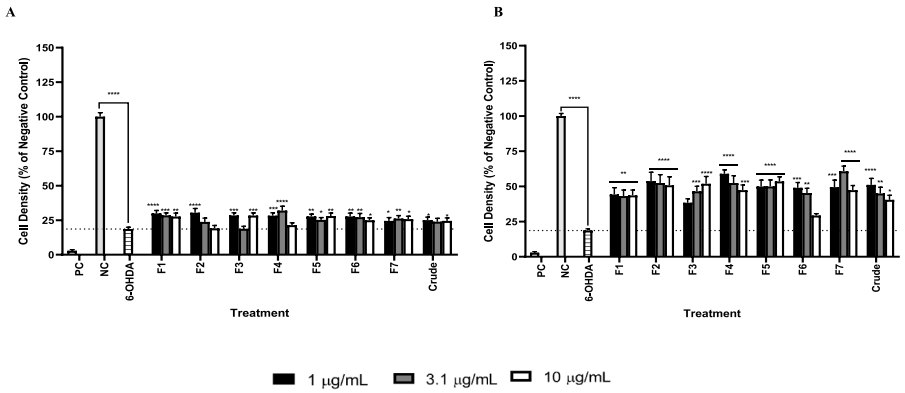

Fig. 4. Cytoprotective effect of *Catha edulis* (A) and *Datura stramonium* (B) crude extracts and fractions (F1 - F7) against 6-hydroxydopamine-induced neurotoxicity in SH-SY5Y cells after 48 h exposure. Values are presented as means ± SEM of three biological and technical repeats (n = 9). Significance relative to 6-OHDA; *p < 0.05, **p < 0.01, ***p < 0.001, ****p < 0.0001. 6-OHDA: 6-hydroxydopamine (72.83 µM), NC: negative control, and PC: positive control (1 % saponin).

generally low, which may be ascribed to the presence of the alkaloid, cathine (Engidawork, 2017). Cathine, although primarily known for its stimulating properties, may have mild cytotoxic effects that could counteract the plant's protective action. Cathine has structural resemblance to other psychoactive drugs such as amphetamine, which has been reported to interfere with various cellular processes, including cell signalling (Paz-Ramos et al., 2023). The observed cytoprotection may therefore reflect a balance between the beneficial properties of *C. edulis'* phenolics and flavonoids, which are potent antioxidants, and the potential toxicity of its alkaloid content.

Datura stramonium crude extract and F3, F4, and F6 demonstrated a dose-dependent increased cell density (Fig. 4B). Fraction 4 increased cell density by 40.32 % ($p < 0.0001$), 33.80 % ($p < 0.0001$), and 28.71 % ($p < 0.001$), at 1, 3.1, and 10 µg/mL, respectively. The lower cytoprotection observed at higher concentrations could be due to the complex interactions between different compounds found in the plant extract, potentially reducing the overall protective effect. Fraction 7 demonstrated the highest cytoprotection at 3.1 µg/mL, with a significant ($p < 0.0001$) increase in cell density of 42.12 %. In contrast, F6 exhibited the lowest cytoprotection at 10 µg/mL, increasing cell density by 10.62 %. This reduced cytoprotection could be due to an additive cytotoxic effect between the inherent phytochemicals and 6-OHDA.

Datura stramonium extracts demonstrated greater cytoprotection at lower concentrations, indicating that intrinsic cytotoxicity may limit their beneficial effects at higher doses. This aligns with the known CNS depressant effects of tropane alkaloids, such as atropine and hyoscyamine, which are neuroprotective at low doses but can cause adverse effects, including sedation and confusion, at higher doses due to their anticholinergic properties (Umarudeen et al., 2023). Although there are no studies that have specifically evaluated the neuroprotective effects of *D. stramonium* extracts on 6-OHDA-induced SH-SY5Y cells, findings from research on *D. inoxia* Mill. offer relevant insights. In that study, lower concentrations of the extract enhanced cell survival in glutamate-induced toxicity, increasing cell density to 77 %, compared to ~49 % viability in the glutamate control group (Vélez-Huerta et al., 2022). These results suggest that *Datura* species, including *D. stramonium*, may exhibit similar neuroprotective effects at lower concentrations, supporting their potential for therapeutic applications in neurodegenerative conditions.

The cytotoxicity and cytoprotection of *C. edulis* and *D. stramonium* crude extracts and fractions on cell density in 6-OHDA-naïve and 6-OHDA-exposed cells after 48 h of treatment is summarised in Table 2.

To further support the cytoprotective results, a qualitative analysis was conducted to observe cell morphology. Under normal cell culture conditions (negative control), SH-SY5Y cells looked healthy, with increased density, and grew as monolayers, characterised by flattened morphology and elongated neurites (data not shown). However, treatment with 6-OHDA resulted in morphological changes; causing the cells to become rounded, lose density, and exhibit impaired neurite formation. These morphological changes are consistent with apoptosis, likely due to the increased caspase-3 activity and elevated Cytochrome *c* (Cyt *c*) levels triggered by 6-OHDA-mediated cell damage (Latchoumycandane et al., 2011).

Mitochondria are central to the process of apoptosis, as stress-induced release of proteins like Cyt *c* into the cytosol activates the caspase-dependent apoptotic cascade (Susin et al., 1999). Gomez-Lazaro et al. (2008) demonstrated that in 6-OHDA-treated SH-SY5Y cells, Cyt *c* is released via the mitochondrial permeability transition (MPT) pore, leading to mitochondrial damage. Similarly, Latchoumycandane et al. (2011) observed that rat dopaminergic neurons exposed to 100 µM 6-OHDA for 3 and 6 h experienced an 80 %–200 % increase in cytosolic Cyt *c* levels, indicating mitochondrial dysfunction linked to 6-OHDA-induced cell death.

Additionally, Moosavi et al. (2018) reported that 6-OHDA treatment in SH-SY5Y cells led to cell body shrinkage, a reduction in the number of living cells, and increased cell debris after 24 h. These findings suggest that 6-OHDA-mediated cell death involves a combination of necrosis and apoptosis (Ju et al., 2010).

Cells treated with either *C. edulis* or *D. stramonium* showed similar morphology (results not shown), with most cells retaining intact, long protruding neurites, which correlates with the cytoprotection results. *C. edulis* exhibited the highest cytoprotective activity at 3.1 µg/mL. In contrast, the lowest concentration (1 µg/mL) of *D. stramonium* showed better cytoprotective activity than 3.1 and 10 µg/mL.

The cell morphology observations support the cytoprotection results. However, cell morphology alone cannot distinguish between cell death by necrosis or apoptosis. Although the exact mechanism of cell death was unclear, both *C. edulis* and *D. stramonium* crude extracts and fractions, managed to increase cell viability, providing a foundation for future research. Preserving the survival of dopaminergic neurons in PD could alleviate the efficiency of currently available treatments.

3.5. Cytotoxicity and cytoprotection of the phytochemical markers

Atropine and scopolamine induced a concentration-dependent effect on cell viability (data not shown). The IC_{50} of atropine was determined as 49.48 µM in the current study, which is in contrast to the IC_{50} of 1.74 µM obtained by Lochner and Thompson (2016). A similar discrepancy was noted for the IC_{50} of scopolamine, 48.26 µM versus 2.09 µM (Lochner and Thompson, 2016). The substantial difference in values is attributed to variations in cell lines, as Lochner and Thompson (2016) used human embryonic kidney cells (HEK293), which exhibit different sensitivity and responses compared to neuroblastoma cells.

Further discrepancies in the IC_{50} values for scopolamine was the IC_{50}

Table 2
A summary of the effect of the crude extract and fractions (F1 - F7) of *Catha edulis* and *Datura stramonium* on cell density in 6-hydroxydopamine-naïve (cytotoxicity) and 6-hydroxydopamine-exposed (cytoprotection) cells after 48 h treatment.

	Cell density (% relative to negative control) (mean ± SEM)									
Plant	Concentration (µg/mL)	Cytotocicity/Cytoprotection	F1	F2	F3	F4	F5	F6	F7	Crude
Catha edulis	1	Cytotoxicity	103.03 ± 1.95	103.84 ± 1.46	95.1 ± 1.54	103.24 ± 1.73	98.37 ± 0.97	102.67 ± 1.58	99.81 ± 1.71	99.74 ± 3.77
		Cytoprotection	29.92 ± 2.13	30.47 ± 3.05	28.4 ± 1.94	28.24 ± 2.14	27.69 ± 1.74	27.21 ± 2.44	24.48 ± 2.46	25.09 ± 2.12
	3.1	Cytotoxicity	99.52 ± 2.01	101.67 ± 2.46	94.43 ± 2.16	99.21 ± 1.30	98.29 ± 1.20	96.05 ± 1.30	101.57 ± 2.52	92.60 ± 2.71
		Cytoprotection	28.53 ± 1.80	23.74 ± 2.75	18.82 ± 1.71	31.99 ± 3.10	25.19 ± 1.74	27.22 ± 2.64	26.20 ± 2.13	23.91 ± 2.45
	10	Cytotoxicity	92.31 ± 2.26	97.80 ± 1.74	99.25 ± 1.32	92.32 ± 2.24	91.37 ± 1.52	87.66 ± 1.84	101.87 ± 1.32	82.1 ± 2.66
		Cytoprotection	27.62 ± 2.52	19.06 ± 2.15	28.32 ± 1.96	21.45 ± 1.55	28.03 ± 2.21	24.98 ± 1.75	25.78 ± 2.09	24.53 ± 2.14
Datura stramonium	1	Cytotoxicity	88.57 ± 5.46	93.62 ± 5.38	82.07 ± 5.19	98.42 ± 4.04	91.61 ± 4.32	96.00 ± 3.64	99.01 ± 3.72	88.96 ± 4.73
		Cytoprotection	44.26 ± 4.86	53.76 ± 6.24	38.36 ± 2.87	58.94 ± 2.77	49.92 ± 4.51	49.05 ± 3.72	49.51 ± 4.97	51.06 ± 4.63
	3.1	Cytotoxicity	83.53 ± 5.32	95.54 ± 7.15	82.38 ± 4.54	94.41 ± 4.06	95.16 ± 3.57	88.60 ± 3.45	101.29 ± 4.66	89.78 ± 4.17
		Cytoprotection	43.12 ± 4.31	52.42 ± 5.95	46.51 ± 3.57	52.42 ± 5.21	49.92 ± 4.72	45.25 ± 3.39	60.74 ± 3.70	44.97 ± 4.43
	10	Cytotoxicity	77.59 ± 4.96	91.19 ± 6.17	85.31 ± 5.61	88.63 ± 8.63	103.06 ± 3.79	90.37 ± 5.03	96.22 ± 3.39	85.25 ± 4.62
		Cytoprotection	43.55 ± 3.85	50.79 ± 6.06	51.83 ± 5.23	47.33 ± 3.65	53.56 ± 3.30	29.24 ± 1.44	47.32 ± 3.27	40.41 ± 3.29

of 2 mM (Suthprasertporn et al., 2020) compared to the IC_{50} of 48.26 µM determined in the current study. Differences across studies may be ascribed to the use of different cytotoxicity assays. The MTT assay measures metabolic activity, while the SRB assay assesses protein content, potentially leading to differing interpretations of cytotoxic effects (Papadimitriou et al., 2019).

Treatment with 6-OHDA alone reduced cell density by 81.38 % (Fig. 5). The observed cell loss is corroborated by findings where 6-OHDA treatment was shown to reduce cell density in neuronal cell lines as discussed earlier (Hanrott et al., 2006).

Atropine and scopolamine significantly ($p < 0.0001$) increased cell density by 30.69 % and 27.88 %, respectively (Fig. 5). It is proposed that both compounds counteract the cytotoxic effects induced by 6-OHDA, likely through their activity as muscarinic receptor antagonists. Alkaloids, in general, are known to exhibit neuroprotective effects by reducing OS, alleviating neuroinflammation, inhibiting cholinesterases, and preventing apoptosis while modulating autophagy (Ali et al., 2023).

In support of the cytoprotective results, cell morphology was visualised and captured (data not shown). Treatment with atropine and scopolamine resulted in a mixed cellular response, with some cells maintaining their elongated morphology and intact neurites, while others exhibited a rounded shape. These observations are consistent with the cytoprotective effects demonstrated in the viability assays, where both compounds preserved cell survival.

The presence of intact cells with neurites indicates that atropine and scopolamine effectively mitigated the neurotoxic effects of 6-OHDA in a subset of the cell population. However, the appearance of some rounded cells may reflect incomplete protection or variability in the extent of cytoprotection.

3.6. Intracellular reactive oxygen species generation

Treatment with 6-OHDA alone increased intracellular ROS generation by 2.82 ± 0.25-fold compared to the negative control (Fig. 6). These findings are in agreement with those obtained in other studies, where 6-OHDA-induced OS was identified as a key contributor to neuronal damage through excessive ROS production (Jaisin et al., 2016; Luo and Sakamoto, 2023; Luo et al., 2022) observed a 1.55 ± 0.10-fold increase in ROS levels when SH-SY5Y cells were treated with 50 µM 6-OHDA for 24 h. Similarly Luo et al. (2022) found that treatment with 75 µM 6-OHDA led to a 2.5-fold increase in ROS compared to the controls. Chen

Fig. 5. The cytoprotective activity of atropine and scopolamine on 6-hydroxydopamine induced cytotoxicity in SH-SY5Y cells. Results are reported as mean ± SEM of three biological and technical repeats (n = 9). Significance is expressed relative to 6-OHDA; ****$p < 0.0001$. 6-OHDA: 6-hydroxydopamine (72.83 µM), NC: negative control, and PC: positive control (1 % saponin).

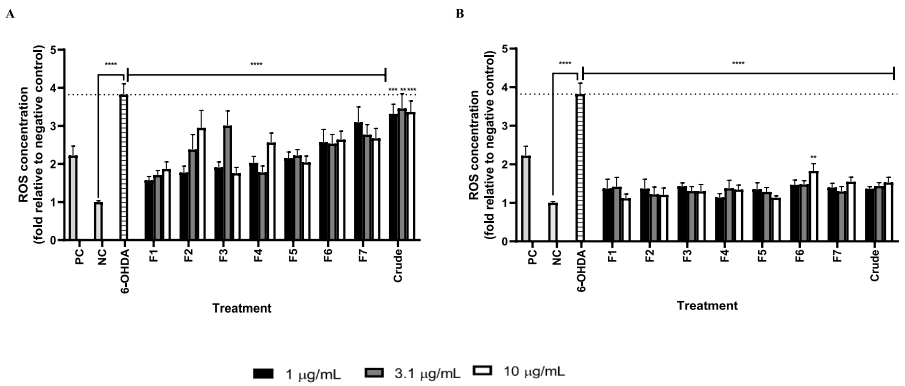

Fig. 6. The effect of *Catha edulis* (A) and *Datura stramonium* (B) crude extract and fractions (F1 - F7) on 6-hydroxydopamine induced reactive oxygen species generation in SH-SY5Y cells. Results are reported as mean ± SEM of three biological and technical repeats (n = 9). Significance is expressed relative to 6-OHDA; **p < 0.01, ***p < 0.001, ****p < 0.0001. 6-OHDA: 6-hydroxydopamine (72.83 µM), ROS: reactive oxygen species, NC: negative control, and PC: positive control (500 µM potassium persulfate).

et al. (2012) reported a 2.3-fold increase in ROS formation after treating SH-SY5Y cells with 100 µM 6-OHDA for 1 h. Also, ROS levels increased 3.7-fold when SH-SY5Y cells were treated with 6-OHDA (Ikeda et al., 2008).

The variation in ROS generation across studies can be attributed to different experimental conditions such as 6-OHDA concentration, exposure duration, and assay type (Luo et al., 2022). Also, in this study, the fluorescence results were normalised to protein content to compensate for changes in cell density caused by cell death (using the SRB assay), a factor that was not considered in the studies conducted by the other authors.

Catha edulis crude extract and fractions significantly ($p < 0.0001$) reduced 6-OHDA-induced ROS generation at all concentrations tested (Fig. 6A). Fraction 7 showed a concentration-dependent decrease, with a significant ($p < 0.0001$) reduction in ROS of 0.73 ± 0.12-fold, 1.05 ± 0.02-fold, and 1.15 ± 0.01-fold for 1, 3.1, and 10 µg/mL, respectively. Fractions 1 and 2 also demonstrated concentration-dependent reductions, with a smaller increase in ROS observed at higher concentrations. Fraction 1 significantly ($p < 0.0001$) reduced ROS by 2.5 ± 0.19-fold, 2.11 ± 0.16-fold, and 1.95 ± 0.1-fold at 1, 3.1, and 10 µg/mL, respectively.

The reduction in ROS levels noted in this study is most likely due to *C. edulis's* antioxidant capabilities. *C. edulis* is reported to contain high concentrations of phenolics and flavonoids, which have strong free radical-scavenging properties (Mohd Sairazi and Sirajudeen, 2020; Sengupta et al., 2011). Abdelwahab et al. (2018) reported a high phenolic and flavonoid content in *C. edulis* , whereas Vinokur (2008) found that *C. edulis* leaves contained high concentrations of polyphenols and ascorbic acid, which will boost antioxidant potential. *Catha edulis* oil extract was shown to possess antioxidant activity (23.5–23.6 µg ascorbic acid equivalent/kg of dry matter) using the 2,2-diphenyl-1-picrylhydrazyl (DPPH) assay (Hailu et al., 2017).

Additional support for these findings is provided by research on other plants rich in phenolic compounds (Noui et al., 2022). investigated *Ephedra alata* subsp. *alenda* Trab., a plant with a biochemical profile similar to *C. edulis,* as both contain ephedrine. *Ephedra alata* subsp. *alenda* demonstrated antioxidant activity in the DPPH assay, with an IC_{50} value of 12.25 ± 1.09 µg/mL, and was also found to have a high total phenolic content of 358.06 ± 10.74 µg gallic acid equivalent (GAE)/mg. These findings emphasise the critical role of phenolic compounds in *C. edulis* in mitigating OS, a key contributor to cellular damage in PD. By lowering ROS levels, *C. edulis* demonstrates potential therapeutic benefits, as reflected in the cytoprotective effects discussed earlier. This implies that the antioxidant properties of *C. edulis* could provide significant advantages in reducing OS linked to the disease (Nataraj et al., 2016).

Datura stramonium crude extract and fractions also significantly reduced 6-OHDA-induced ROS generation at all concentrations tested (Fig. 6B). Fractions 2, 3, and 5 exhibited concentration-dependent reductions in ROS, with increasing concentrations leading to further decreases in ROS generation. The crude extract and F6 also showed a concentration-dependent reduction in ROS, although higher concentrations, displayed a slight increase in ROS generation. These findings may be attributed to the phenolic and flavonoid content of *D. stramonium.* Al-Snafi (2017) reported the presence of alkaloids, flavonoids, phenols, and glycosides in a methanol extract of *D. metel* L, a species closely related to *D. stramonium* L. Similarly, the methanol extract of *D. metel* was found to effectively inhibit DPPH radicals at concentrations of 5 and 10 µg/mL (Matcha et al., 2013). Furthermore, the methanol extract of *D. inoxia* seeds possessed a high phenolic acid content (268.6 µg GAE/mg of dried sample), indicative of its antioxidant capabilities (Roy et al., 2016).

One of the compounds identified in *D. stramonium,* is noradrenaline, also known as norepinephrine. Norepinephrine is reported to protect neurons against OS induced in SH-SY5Y cells by increasing the supply of GSH from astrocytes via β3-adrenoceptor stimulation (Luo and Sakamoto, 2023). Glutathione is one of the most important antioxidants synthesised in cells and is known to neutralise free radicals, further supporting the ROS-reducing effects observed in *D. stramonium* extracts (Forman et al., 2009).

Based on these assays, a concentration of 3.1 µg/mL for both plants was chosen for subsequent mechanistic studies. This concentration was selected because, despite the absence of a clear dose–response trend, it consistently demonstrated cytoprotective effects across multiple fractions. It also served as a balanced midpoint between the lower dose (1 µg/mL), which was less effective, and the higher dose (10 µg/mL), which produced more variable or potentially cytotoxic effects. The selection of this concentration, provides a balanced approach for subsequent investigations, avoiding the confounding effects seen at higher concentrations and allowing for clearer insights into the underlying mechanisms.

3.7. Apoptosis

6-Hydroxydopamine is known to induce apoptosis primarily by activating caspase-3 (Jaisin et al., 2016). The activation of caspase-3 in PD is strongly associated with neuronal death (Liu et al., 2013; Tatton et al., 2003). The release of Cyt *c* from mitochondria facilitates this process, further linking mitochondrial dysfunction to neurodegeneration (Meng et al., 2025).

Cisplatin is known to induce apoptosis in neuronal cells (Rathinam et al., 2015) and this was confirmed by the significant increase in

caspase 3/7 activity noted (Fig. 7). Similarly, treatment with 6-OHDA alone significantly ($p < 0.0001$) increased caspase 3/7 activity by 4.13 ± 0.07-fold when compared to the negative control (Fig. 7). This finding is supported by Jaisin et al. (2016) who reported a 2.0 ± 0.11-fold increase in caspase-3 activity in SH-SY5Y cells treated with 50 μM 6-OHDA. Treatment of human dopaminergic cells with 75 μM 6-OHDA resulted in a significant increase in cell death with cleaved caspase-3 protein levels being ~25-fold higher than the control group (Luo et al., 2022). These results confirm that 6-OHDA induces caspase-3 activity.

Catha edulis crude extract and fractions also significantly ($p < 0.0001$) reduced caspase 3/7 activity (Fig. 7A). Fraction 4 exhibited the highest reduction in caspase 3/7 activity of 2.16 ± 0.01-fold, possibly indicating a phytochemical profile that enhances its anti-apoptotic properties. The variability in caspase 3/7 reduction may be attributed to differences in the phytochemical composition of the fractions, as *C. edulis* is rich in phenolic compounds, flavonoids, and alkaloids, all known for their antioxidant and anti-apoptotic properties (Abdelwahab et al., 2018). The reduction in caspase 3/7 activity observed in this study is corroborated, where it is suggested that flavonoids inhibit caspase activation and protect against OS-related apoptosis (White et al., 2012). In PD models, OS, triggered by agents like 6-OHDA, leads to increased ROS generation and activation of the apoptotic pathway, including the caspase cascade (Smith and Cass, 2007). The reduction in ROS generation previously observed with *C. edulis* extracts likely contributes to the decreased caspase 3/7 activity, which is consistent with research demonstrating that alleviating OS can prevent apoptotic cell death (Kannan and Jain, 2000).

The crude extract and fractions of *D. stramonium* significantly ($p < 0.0001$) reduced caspase 3/7 activity (Fig. 7B). The crude extract and F1, F3, and F6 demonstrated virtually equivalent reductions in caspase 3/7 activity, indicating that the phytochemicals responsible for this inhibition are present throughout. Notably, Fraction 7 showed the highest reduction in caspase 3/7 activity of 3.66 ± 0.05-fold, suggesting a higher concentration of active compounds in this fraction.

The notable reduction in caspase 3/7 activity aligns with research highlighting the anti-apoptotic properties of the phytochemical compounds, such as alkaloids, flavonoids, and phenolics in *D. stramonium* (Sharma et al., 2021). *Datura stramonium* is known for its therapeutic and neuroprotective effects, which are attributed to its phenolic compounds and flavonoids (Soni et al., 2012). These compounds possess the ability to scavenge free radicals, preserve cellular integrity, and mitigate OS and apoptosis, thereby enhancing their therapeutic potential (Roy et al., 2022).

The observed reduction in caspase 3/7 activity indicates that *C. edulis* and *D. stramonium* may hold therapeutic potential in safeguarding neuronal cells from OS-induced apoptosis, a key feature of PD. Both plant extracts seem to reduce apoptosis by inhibiting caspase 3/7 activity, likely by decreasing OS and in turn, preventing the activation of apoptotic pathways linked to cellular damage. However, *D. stramonium* demonstrated a more pronounced reduction in caspase 3/7 activity, suggesting a stronger neuroprotective effect. These findings highlight the potential of these extracts as neuroprotective agents.

3.8. Mitochondrial integrity

Potassium persulfate, an oxidising agent, induces OS and generates ROS, disrupting the mitochondrial membrane potential (MMP), impairing ATP production, and potentially opening the MPT pore. This mitochondrial damage is reflected by an increased ratio of damaged mitochondria to cell density (Fig. 8). Similarly, 6-OHDA treatment increased fluorescence intensity, indicating significant mitochondrial damage, and reduced cell density. After normalising fluorescence to cell density, the 6-OHDA-treated group showed a 0.50 ± 0.3 increase in the ratio of healthy mitochondria to cell density compared to the control, indicating greater mitochondrial damage. These results align with findings by Silva et al. (2018), where treatment of SH-SY5Y cells with 100 μM 6-OHDA caused significant MMP depolarisation. Similarly, Shih et al. (2011) reported that 100 μM 6-OHDA induced approximately 70 % MMP depolarisation in SH-SY5Y cells.

The self-oxidation of DA to 6-OHDA produces free radicals and unstable quinones, which trigger the oxidation of lipids and damage to the mitochondrial membrane. This damage ultimately leads to the disintegration of the MMP, which causes cell death (Hanrott et al., 2006). A correlation exists between MMP depolarisation and ROS production, as well as MMP depolarisation and neuronal death.

The crude extract and fractions of *C. edulis* demonstrated the ability to preserve mitochondrial integrity, as indicated by the significant reduction in the ratio of healthy mitochondria to cell density (Fig. 8A). The crude extract and F1 to F5 showed a relatively consistent protective effect. Fraction 6 demonstrated the most significant reduction in the ratio, decreasing it by 0.82 ± 0.26 ($p < 0.001$), suggesting a stronger ability to maintain mitochondrial integrity, possibly due to a higher concentration of protective bioactive compounds or a unique combination of phytochemicals.

Similarly, *D. stramonium* extracts and fractions also maintained mitochondrial integrity (Fig. 8B), reducing the ratio of healthy mitochondria to cell density. Fractions 1, 3, and 5 displayed similar and significant ($p < 0.001$) reductions in the ratio of healthy mitochondria to cell density. The crude extract showed the most significant reduction in the ratio of healthy mitochondria to cell density, decreasing it by 1.08 ± 0.29 ($p < 0.0001$), thus indicating its potential to protect against mitochondrial disruption.

The mitochondrial integrity observed for *D. stramonium* in this study might be attributed to its antioxidant activity, hence mitigating OS and preventing mitochondrial impairment. Co-incubation of the methanol extract of *Hyoscyamus niger* L. with MPP^+, which is known to induce mitochondrial dysfunction, significantly reduced the generation of hydroxyl radicals (Sengupta et al., 2011). This reduction in ROS may have contributed to preserving mitochondrial function. Additionally, given

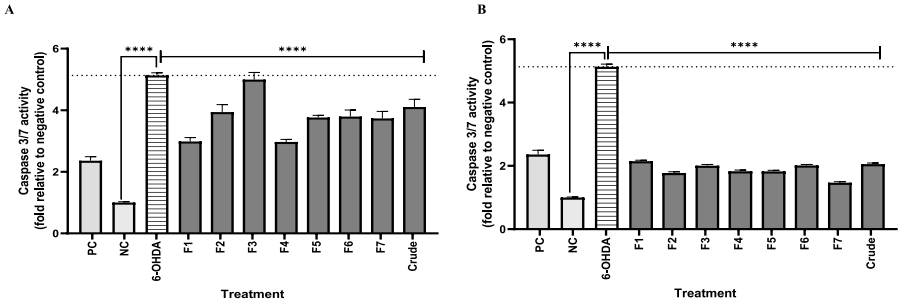

Fig. 7. The effect of *Catha edulis* (A) and *Datura stramonium* (B) crude extract and fractions (3.1 μg/mL) on 6-hydroxydopamine induced caspase 3/7 activity. Results are reported as mean ± SEM of three biological and technical repeats (n = 9). Significance is expressed relative to 6-OHDA; ****$p < 0.0001$. 6-OHDA: 6-hydroxydopamine (72.83 μM), NC: negative control, and PC: positive control (29.85 μM cisplatin).

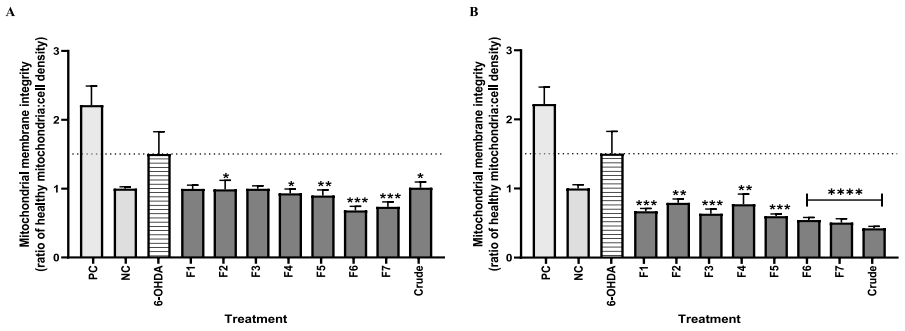

Fig. 8. The effect of *Catha edulis* (A) and *Datura stramonium* (B) crude extract and fractions (3.1 μg/mL) on mitochondrial membrane integrity. Results were reported as mean ± SEM of three biological and technical repeats (n = 9). Significance is expressed relative to 6-OHDA; *p < 0.05, **p < 0.01, ***p < 0.001, ****p < 0.0001. 6-OHDA: 6-hydroxydopamine (72.83 μM), NC: negative control, and PC: positive control (1 mM potassium persulfate).

that *D. stramonium* contains phenolic and flavonoid compounds with significant antioxidant potential, it is likely that its protective effects are mediated through similar mechanisms, emphasising its role in reducing OS and preserving mitochondrial integrity.

The reduction in mitochondrial damage caused by *C. edulis* and *D. stramonium* fractions is of importance, as mitochondrial dysfunction is a key factor in cell death, particularly in PD (Keane et al., 2011). By safeguarding mitochondrial integrity, fractions of *C. edulis* and *D. stramonium* may help reduce OS and apoptosis, as evidenced by the observed decrease in ROS levels and caspase activity. The rich phytochemical content of both plants, which includes alkaloids, flavonoids, and phenolics, likely contributes to this effect by scavenging ROS and preventing mitochondrial membrane collapse, supporting their role in enhancing mitochondrial stability under oxidative conditions (Koklesova et al., 2021). These results align with literature on plant-derived compounds, such as flavonoids and phenolic compounds, which are known for stabilising mitochondrial membranes and preventing dysfunction under oxidative conditions (Koklesova et al., 2021).

The established link between mitochondrial dysfunction, OS, and apoptosis in PD suggests that *C. edulis* and *D. stramonium* crude extracts and fractions could be valuable for therapeutic interventions aimed at maintaining mitochondrial function and preventing cell death. Both *C. edulis* and *D. stramonium* extracts play a protective role in maintaining mitochondrial integrity, potentially mitigating the cellular damage induced by OS and apoptotic signalling pathways. This maintenance of mitochondrial health is essential, as it reduces the likelihood of cell death and helps maintain overall cellular function.

3.9. In silico docking

The free energies calculated from the docking studies revealed higher binding affinities of norephedrine than cathine for both D1 and D2 receptors (Table 3). The binding free energy values of norephedrine for D1 and D2 were −4.34 kJ/mol and −5.91 kJ/mol, respectively, whereas the values for cathine were −3.9 kJ/mol and −5.31 kJ/mol, for D1 and D2, respectively. Norephedrine has a higher binding affinity, especially for the D2 receptor, as indicated by its lower (more negative) binding free energy values. The relatively higher predicted affinity of norephedrine for the D2 receptor is noteworthy, as modulation of D2-mediated dopaminergic signalling is a major therapeutic target in PD (Du et al., 2016; Isaacson et al., 2023). However, it is important to note that these results reflect *in silico* predictions of receptor-ligand affinity, and do not confirm functional agonist or antagonist activity. Further experimental validation using receptor activation assays is required to determine the true pharmacological effects of these compounds. The docking poses and 2D ligand-protein interaction diagrams for each compound at the D1 and D2 receptors is depicted in Table 3. The results indicate that apomorphine, a known D1 receptor agonist (Lees, 1993), primarily formed interactions via π-π stacking, hydrogen bonding, and a salt bridge. In contrast, cathine and norephedrine formed distinct binding interactions, with cathine forming a hydrogen bond and norephedrine forming a salt bridge to specific amino acid residues. Notably, both compounds shared only one common amino acid residue with apomorphine, suggesting a different binding orientation that may influence their functional efficacy at the D1 receptor (Zhuang et al., 2021).

Similarly, in the D2 receptor, risperidone, a well-known antagonist (Wang et al., 2018), predominantly formed interactions via π-π stacking, hydrogen bonding, and a salt bridge (Table 3). Norephedrine shares several amino acid residues with risperidone, suggesting similar binding modes and supporting its potential as a D2 receptor modulator. In contrast, cathine formed a hydrogen bond to a unique amino acid residue, indicating a slightly different binding configuration. This variation could impact cathine's binding efficiency and functional activity at the D2 receptor (Kalyanasundar et al., 2020).

Cathine and norephedrine interacted with dopaminergic modulators at activator sites, including apomorphine at the D1 receptor and risperidone at the D2 receptor. These interactions suggest their potential to influence receptor activity through distinct binding mechanisms. Given the critical role of D2 receptors in motor control pathways disrupted by DA deficiency in PD, norephedrine's strong binding to these receptors suggests it could mimic DA's effects or modulate receptor activity (Aoyama et al., 2000). This potential to alleviate motor symptoms positions norephedrine as a compelling candidate for further research into treatments targeting dopaminergic pathways (Fox and Lang, 2010). Notably, D2 agonists play a key role in relieving motor symptoms in PD by modulating the disrupted indirect pathway of the basal ganglia (Jenner, 1995). However, its promise as a treatment requires a cautious and thorough evaluation, particularly in understanding its specificity, efficacy, and safety in restoring dopaminergic signalling in PD patients.

The molecular docking assessment of compounds present in *D. stramonium* (atropine, hyoscyamine, and noradrenaline) within the D1 and D2 receptors showed notable differences in binding affinities (Table 4). The highest binding affinity to both receptors was shown by noradrenaline, which displayed free energy values of −6.73 kJ/mol for D1 and -7.43 kJ/mol for D2. In contrast, both atropine and hyoscyamine displayed lower affinities; atropine binds with a binding free energy of −4.55 kJ/mol for D1 and -4.31 kJ/mol for D2, and hyoscyamine with energy values of −5.54 kJ/mol for D1 and -4.34 kJ/mol for D2.

The specific binding affinity of noradrenaline to D1 and D2 receptors may be crucial for PD treatment, as noradrenaline is essential for motor control and neuronal function (Fornai et al., 2007). In PD, noradrenaline is deficient, contributing to worsening symptoms and dyskinesia, which are commonly seen in PD patients during DA replacement therapy (Fornai et al., 2007). The high receptor binding affinity of noradrenaline suggests its potential to activate DA receptors, which could enhance its signalling pathways.

By stimulating both D1 and D2 receptors, noradrenaline may boost DA cell activity and mitigate the effects of DA deficiencies. Additionally,

Table 3
Binding affinity of compounds identified in *Catha edulis* for dopamine receptors D1 (PDB: 7JVQ) and D2 (PDB: 6CM4).

Dopamine receptor	Ligand	Ligand-interaction	Common residues	Other residues	Affinity (KJ/mol)
D1 Receptor	Apomorphine	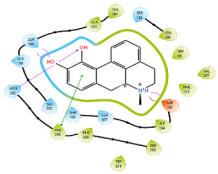	ASN292, ASP103, PHE289, and SER198	–	–
	Cathine	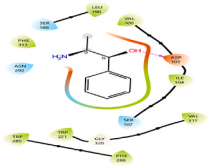	ASP103	–	−3.9
	Norephedrine	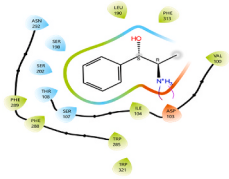	ASP103	–	−4.34
D2 receptor	Risperidone	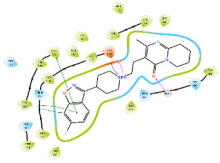	ASP114, H_2O, PHE390, and TRP386	–	–
	Cathine	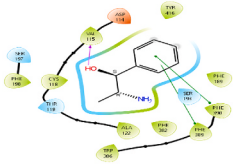	PHE390, and TRP386	VAL115	−5.31
	Norephedrine	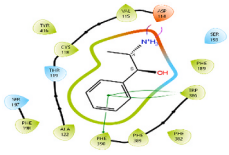	ASP114, PHE390, and TRP386	–	−5.91

Key

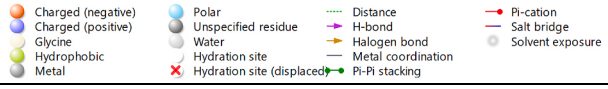

the restoration of noradrenergic activity has been shown to reduce dyskinesia, a common side effect of PD treatment (Fornai et al., 2007). Given these effects, noradrenaline's strong affinity for these receptors supports additional research into its therapeutic potential in regulating motor activities and potentially alleviating some of the side effects associated with current treatments.

All compounds formed interactions with the receptor binding site through π-π stacking, hydrogen bonding, and salt bridges (Table 4), which are critical for stabilising ligand-receptor complexes, as demonstrated by the reference compound, apomorphine (Durdagi et al., 2016; Jóźwiak and Płazińska, 2021). Atropine and hyoscyamine both formed salt bridge interactions, while noradrenaline demonstrated multiple interactions, including hydrogen bonding and π-π stacking, with several amino acid residues. This similarity in binding mechanisms highlights noradrenaline's strong affinity for the D1 receptor, suggesting its potential to achieve receptor activation comparable to that of the reference ligand.

Atropine formed a distinct hydrogen bond to the receptor binding site, while hyoscyamine formed both a hydrogen bond and a π-cation interaction stabilised by specific amino acid residues. Similarly, noradrenaline exhibited a hydrogen bond with a specific amino acid residue, potentially enhancing its binding affinity. These interactions highlight the unique binding mechanisms of each compound, which could play an important role in determining their efficacy in modulating D1 receptor activity (Jóźwiak and Płazińska, 2021).

Similar to the D1 receptor, interactions with the D2 receptor were mediated by π-π stacking, hydrogen bonding, and salt bridges. Hyoscyamine formed a hydrogen bond interaction, while noradrenaline formed a π-π stacking interaction and a salt bridge, both stabilised by key amino acid residues. These interactions suggest that these compounds may

Table 4
Binding affinity of compounds identified in *Datura stramonium* for dopamine receptors D1 (PDB: 7JVQ) and D2 (PDB: 6CM4).

Dopamine receptor	Ligand	Ligand-interaction	Common residues	Other residues	Affinity (KJ/mol)
D1 receptor	Apomorphine	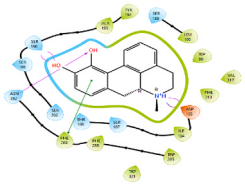	ASN292, ASP103, PHE289, and SER198	–	–
	Atropine	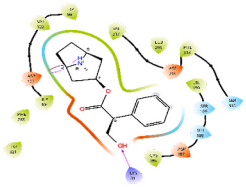	ASP103	LYS81	−4.55
	Hyoscyamine	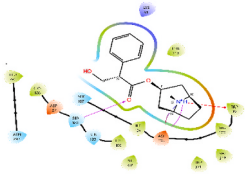	ASP103	SER188 and TRP99	−5.54
	Noradrenaline	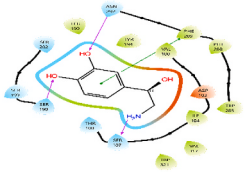	ASN292, PHE289, and SER198	SER107	−6.73
D2 receptor	Risperidone	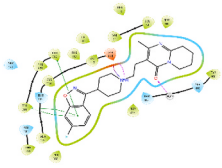	ASP114, H_2O, PHE390, and TRP386	–	–
	Atropine	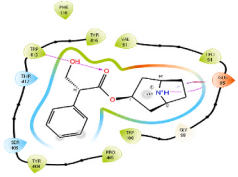	–	GLU95 and TRP413	−4.31
	Hyoscyamine	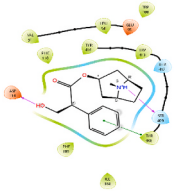	ASP114	SER409 and TYR408	−4.34
	Noradrenaline	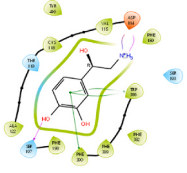	ASP114, PHE390, and TRP386	SER197	−7.43

Key: refer to Table 3.

bind to the D2 receptor in a manner similar to risperidone. The close resemblance of noradrenaline's binding mode to that of risperidone likely explains its higher binding affinity and supports its potential role as a D2 receptor modulator. Noradrenaline has higher affinity for D1 and D2 receptors because of its structural similarity with DA (Senior et al., 2020). Both compounds are catecholamines and share a common core structure; a catechol group and an amine group (Fitzgerald, 2021). The main difference between the two is the additional hydroxyl group on the β-carbon of noradrenaline. This similarity in the structural framework allows noradrenaline to interact with DA receptors more effectively than other compounds.

In contrast, atropine formed both hydrogen bond and salt bridge interactions, while hyoscyamine formed a hydrogen bond and a π-π stacking interaction, stabilised by unique amino acid residues. Noradrenaline, on the other hand, formed a hydrogen bond with a specific amino acid residue. These specific interactions suggest that, although hyoscyamine and noradrenaline share general binding features, their exact positioning and interaction with the receptor differ, potentially influencing their therapeutic outcomes and receptor modulation capabilities (Jóźwiak and Płazińska, 2021).

Norephedrine and noradrenaline emerged as the most promising compounds in *C. edulis* and *D. stramonium*, respectively, exhibiting the highest binding affinities for D1 and D2 receptors. This suggests their potential as dual-acting agonists of DA receptors. The distinct interactions observed for each compound indicates variations in their binding modes, which could influence their pharmacological response and therapeutic applications. These findings provide a strong foundation for further *in vitro* and *in vivo* studies to explore the potential of noradrenaline, particularly in the treatment of neurodegenerative disorders such as PD.

4. Conclusion

Catha edulis and *D. stramonium* extracts show promising therapeutic potential for PD. Their minimal cytotoxicity, cytoprotective properties, and ability to reduce OS suggest they may protect against neuronal damage. The extracts also appear to inhibit apoptosis by reducing caspase 3/7 activity and maintaining mitochondrial integrity, which are critical for slowing neurodegeneration in PD. Additionally, the affinity of norephedrine and noradrenaline for dopamine receptors indicates potential for restoring dopamine function, alleviating motor symptoms. While further *in vivo* studies are needed, these findings provide a strong foundation for future research into their as potential therapeutic agents for PD.

CRediT authorship contribution statement

T. Mogale: Writing – original draft, Investigation, Formal analysis. **A.D. de Beer:** Writing – review & editing, Supervision. **W.J. Rudolph:** Writing – review & editing, Methodology. **V. Steenkamp:** Writing – review & editing, Supervision, Conceptualization.

Declaration of competing interest

The authors declare that they have no known competing financial interests or personal relationships that could have appeared to influence the work reported in this paper.

Acknowledgments

The authors gratefully acknowledge the National Research Foundation for funding (Grant Number: PMDS2205046492), the Department of Chemistry at the University of Pretoria for providing the plant samples, and the Biodiscovery Group, Department of Chemistry, University of Pretoria, for mass spectrometry analysis.

Appendix A. Supplementary data

Supplementary data to this article can be found online at https://doi.org/10.1016/j.jep.2026.121223.

Data availability

Data will be made available on request.

References

Abdelwahab, S.I., Alsanosy, R., Mohamed Elhassan Taha, M., Mohan, S., 2018. Khat-induced toxicity: role in its modulating effects on inflammation and oxidative stability. BioMed Res. Int. 2018 (1), e5896041. https://doi.org/10.1155/2018/5896041.

Afsheen, N., Rafique, S., Rafeeq, H., Irshad, K., Hussain, A., Huma, Z., Kumar, V., Bilal, M., Aleya, L., Iqbal, H.M., 2022. Neurotoxic effects of environmental contaminants—measurements, mechanistic insight, and environmental relevance. Environ. Sci. Pollut. Res. 29 (47), 70808–70821. https://doi.org/10.1007/s11356-022-22779-2.

Afzal, S., Abdul Manap, A.S., Attiq, A., Albokhadaim, I., Kandeel, M., Alhojaily, S.M., 2023. From imbalance to impairment: the central role of reactive oxygen species in oxidative stress-induced disorders and therapeutic exploration. Front. Pharmacol. 14, e1269581. https://doi.org/10.3389/fphar.2023.1269581.

Agu, P., Afiukwa, C., Orji, O., Ezeh, E., Ofoke, I., Ogbu, C., Ugwuja, E., Aja, P., 2023. Molecular docking as a tool for the discovery of molecular targets of nutraceuticals in diseases management. Sci. Rep. 13 (1), e13398. https://doi.org/10.1038/s41598-023-40160-2.

Al-Snafi, A.E., 2017. Medical importance of *Datura fastuosa* (syn: *Datura metel*) and *Datura stramonium*—A review. IOSR J. Pharm. 7 (2), 43–58. https://doi.org/10.9790/3013-0702014358.

Al-Motarreb, A., Baker, K., Broadley, K.J., 2002. Khat: pharmacological and medical aspects and its social use in Yemen. Phytother Res. 16 (5), 403–413. https://doi.org/10.1002/ptr.1106.

Alfaifi, H., Abdelwahab, S.I., Mohan, S., Taha, M.M.E., Syame, S.M., Shaala, L.A., Alsanosy, R., 2017. *Catha edulis* Forsk. (Khat): evaluation of its antidepressant-like activity. Pharmacogn. Mag. 13 (Suppl. 2), S354. https://doi.org/10.4103/pm.pm_442_16.

Ali, A., Martins, A.M.C., Alam, W., Khan, H., 2023. Neuroprotective effects of alkaloids. In: Phytonutrients and Neurological Disorders: Therapeutic and Toxicological Aspects, pp. 245–257. https://doi.org/10.1016/B978-0-12-824467-8.00001-2.

Ali, W.M., Al Habib, K., Al-Motarreb, A., Singh, R., Hersi, A., Al Faleh, H., Asaad, N., Al Saif, S., Almahmeed, W., Sulaiman, K., 2011. Acute coronary syndrome and khat herbal amphetamine use: an observational report. Circulation 124 (24), 2681–2689. https://doi.org/10.1161/CIRCULATIONAHA.111.039768.

Antoine Lanfranchi, D.A., Tomi, F., Casanova, J., 2010. Enantiomeric differentiation of atropine/hyoscyamine by 13C NMR spectroscopy and its application to *Datura stramonium* extract. Phytochem. Anal. 21 (6), 597–601. https://doi.org/10.1002/pca.1240.

Aoyama, S., Kase, H., Borrelli, E., 2000. Rescue of locomotor impairment in dopamine D2 receptor-deficient mice by an adenosine A2A receptor antagonist. J. Neurosci. 20 (15), 5848–5852. https://doi.org/10.1523/JNEUROSCI.20-15-05848.2000.

Bloem, B.R., Okun, M.S., Klein, C., 2021. Parkinson's disease. Lancet 397 (10291), 2284–2303. https://doi.org/10.1016/S0140-6736(21)00218-X.

Brubacher, J.L., Bols, N.C., 2001. Chemically de-acetylated 2',7'-dichlorodihydrofluorescein diacetate as a probe of respiratory burst activity in mononuclear phagocytes. J. Immunol. Methods 251 (1–2), 81–91. https://doi.org/10.1016/S0022-1759(01)00308-8.

Bussmann, R.W., Paniagua-Zambrana, N.Y., Njoroge, G.N., 2020. *Datura stramonium L.* Solanaceae. Ethnobot. Mt. Reg. Afr. 1-9. https://doi.org/10.1007/978-3-319-77086-4_62-1.

Cetin, S., Knez, D., Gobec, S., Kos, J., Pišlar, A., 2022. Cell models for Alzheimer's and Parkinson's disease: at the interface of biology and drug discovery. Biomed. Pharmacother. 149, 112924. https://doi.org/10.1016/j.biopha.2022.112924.

Chen, X., Guo, C., Kong, J., 2012. Oxidative stress in neurodegenerative diseases. Neural Regen. Res. 7 (5), 376–385. https://doi.org/10.3969/j.issn.1673-5374.2012.05.009.

Cordier, W., Steenkamp, V., 2018. Bulb extracts of Boophone disticha induce hepatotoxicity by perturbing growth, without significantly impacting cellular viability. S. Afr. J. Bot. 114, 1–8. https://doi.org/10.1016/j.sajb.2017.10.005.

Cui, J., Zhao, S., Li, Y., Zhang, D., Wang, B., Xie, J., Wang, J., 2021. Regulated cell death: discovery, features and implications for neurodegenerative diseases. Cell Commun. Signal. 19 (1), 120. https://doi.org/10.1186/s12964-021-00799-8.

Dhabbah, A.M., Badjah-Hadj-Ahmed, A.Y., Alawi, A.I., Al Angari, W.A., Alrayes, B.F., 2018. Screening of psychoactive components in fresh khat using direct analysis in real time-time of flight-mass spectrometry. Saudi J. Forensic Med. Sci. 1 (3), 45–50. https://doi.org/10.4103/sjfms.sjfms_2_19.

Dhuriya, Y.K., Sharma, D., 2018. Necroptosis: a regulated inflammatory mode of cell death. J. Neuroinflammation 15 (1), 199. https://doi.org/10.1186/s12974-018-1235-0.

Dong-Chen, X., Yong, C., Yang, X., Chen-Yu, S., Li-Hua, P., 2023. Signaling pathways in Parkinson's disease: molecular mechanisms and therapeutic interventions. Signal Transduct. Target. Ther. 8 (1), 73. https://doi.org/10.1038/s41392-023-01353-3.

Dorszewska, J., Kowalska, M., Prendecki, M., Piekut, T., Kozłowska, J., Kozubski, W., 2021. Oxidative stress factors in Parkinson's disease. Neural Regen. Res. 16 (7), 1383–1391. https://doi.org/10.3390/antiox9070597.

Du, X., Li, Y., Xia, Y.-L., Ai, S.-M., Liang, J., Sang, P., Ji, X.-L., Liu, S.-Q., 2016. Insights into protein–ligand interactions: mechanisms, models, and methods. Int. J. Mol. Sci. 17 (2), 144. https://doi.org/10.3390/ijms17020144.

Durdagi, S., Salmas, R.E., Stein, M., Yurtsever, M., Seeman, P., 2016. Binding interactions of dopamine and apomorphine in D2 High and D2 low states of human dopamine D2 receptor using computational and experimental techniques. ACS Chem. Neurosci. 7 (2), 185–195. https://doi.org/10.1021/acschemneuro.5b00271.

Engidawork, E., 2017. Pharmacological and toxicological effects of *Catha edulis* F. (Khat). Phytother Res. 31 (7), 1019–1028. https://doi.org/10.1002/ptr.5832.

Erekat, N.S., 2018. Apoptosis and its Role in Parkinson's Disease. Exon Publ, pp. 65–82. https://doi.org/10.15586/codonpublications.parkinsonsdisease.2018.ch4.

Falkenburger, B.H., Saridaki, T., Dinter, E., 2016. Cellular models for Parkinson's disease. J. Neurochem. 139, 121–130. https://doi.org/10.1111/jnc.13618.

Fitzgerald, P.J., 2021. Many drugs of abuse May be acutely transformed to dopamine, norepinephrine and epinephrine *In Vivo*. Int. J. Mol. Sci. 22 (19), 10706. https://doi.org/10.3390/ijms221910706.

Forman, H.J., Zhang, H., Rinna, A., 2009. Glutathione: overview of its protective roles, measurement, and biosynthesis. Molec. Aspects Med. 30 (1–2), 1–12. https://doi.org/10.1016/j.mam.2008.08.006.

Fornai, F., di Poggio, A.B., Pellegrini, A., Ruggieri, S., Paparelli, A., 2007. Noradrenaline in Parkinson's disease: from disease progression to current therapeutics. Curr. Med. Chem. 14 (22), 2330–2334. https://doi.org/10.2174/092986707781745550.

Fox, S., Lang, A.E., 2010. Therapy of the motor features of Parkinson's Disease. Blue Books Neurol. 34, 252–272. https://doi.org/10.1016/B978-1-4160-6641-5.00015-5. Elsevier.

Friesner, R.A., Banks, J.L., Murphy, R.B., Halgren, T.A., Klicic, J.J., Mainz, D.T., Repasky, M.P., Knoll, E.H., Shelley, M., Perry, J.K., 2004. Glide: a new approach for rapid, accurate docking and scoring. 1. Method and assessment of docking accuracy. J. Med. Chem. 47 (7), 1739–1749. https://doi.org/10.1021/jm0306430.

Getasetegn, M., 2016. Chemical composition of Catha edulis (khat): a review. Phytochem. Rev. 15, 907–920. https://doi.org/10.1007/s11101-015-9435-z.

Gomez-Lazaro, M., Galindo, M.F., Concannon, C.G., Segura, M.F., Fernandez-Gomez, F. J., Llecha, N., Comella, J.X., Prehn, J.H., Jordan, J., 2008. 6-Hydroxydopamine activates the mitochondrial apoptosis pathway through p38 MAPK-mediated, p53-independent activation of Bax and PUMA. J. Neurochem. 104 (6), 1599–1612. https://doi.org/10.1111/j.1471-4159.2007.05115.x.

Hailu, Y.M., Atlabachew, M., Chandravanshi, B.S., Redi-Abshiro, M., 2017. Composition of essential oil and antioxidant activity of Khat (*Catha edulis* Forsk), Ethiopia. Chem. Int. 3 (1), 25.

Hajibabaie, F., Abedpoor, N., Mohamadynejad, P., 2023. Types of cell death from a molecular perspective. Biology 12 (11), 1426. https://doi.org/10.3390/biology12111426.

Hanrott, K., Gudmunsen, L., O'Neill, M.J., Wonnacott, S., 2006. 6-hydroxydopamine-induced apoptosis is mediated via extracellular auto-oxidation and caspase 3-dependent activation of protein kinase Cδ. J. Biol. Chem. 281 (9), 5373–5382.

Ikeda, Y., Tsuji, S., Satoh, A., Ishikura, M., Shirasawa, T., Shimizu, T., 2008. Protective effects of astaxanthin on 6-hydroxydopamine-induced apoptosis in human neuroblastoma SH-SY5Y cells. J. Neurochem. 107 (6), 1730–1740. https://doi.org/10.1111/j.1471-4159.2008.05743.x.

Invernizzi, L., Moyo, P., Cassel, J., Isaacs, F.J., Salvino, J.M., Montaner, L.J., Tietjen, I., Maharaj, V., 2022. Use of hyphenated analytical techniques to identify the bioactive constituents of Gunnera perpensa L., a South African medicinal plant, which potently inhibit SARS-CoV-2 spike glycoprotein–host ACE2 binding. Anal. Bioanal. Chem. 414 (13), 3971–3985. https://doi.org/10.1007/s00216-022-04041-3.

Isaacson, S.H., Hauser, R.A., Pahwa, R., Gray, D., Duvvuri, S., 2023. Dopamine agonists in Parkinson's disease: impact of D1-like or D2-like dopamine receptor subtype selectivity and avenues for future treatment. Clin. Park. Relat. Disord. 100–212. https://doi.org/10.1016/j.prdoa.2023.100212.

Jaisin, Y., Ratanachamnong, P., Prachayasittikul, S., Watanapokasin, R., Kuanpradit, C., 2016. Protective effects of ethyl acetate extract of *Eclipta prostrata* against 6-hydroxydopamine-induced neurotoxicity in SH-SY5Y cells. Sci. Asia 42, 259. https://doi.org/10.2306/scienceasia1513-1874.2016.42.259.

Jakabová, S., Vincze, L., Farkas, Á., Kilár, F., Boros, B., Felinger, A., 2012. Determination of tropane alkaloids atropine and scopolamine by liquid chromatography–mass spectrometry in plant organs of *Datura* species. J. Chromatogr. A. 1232, 295–301. https://doi.org/10.1016/j.chroma.2012.02.036.

Jenner, P., 1995. The rationale for the use of dopamine agonists in Parkinson's disease. Neurology 45 (3_Suppl. l_3), S6–S12. https://doi.org/10.1212/WNL.45.3.

Jiang, Q., Yin, J., Chen, J., Ma, X., Wu, M., Liu, G., 2020. Mitochondria-targeted antioxidants: A step towards disease treatment. Oxidative Medicine and Cellular Longevity 2020 (1), 8837893. https://doi.org/10.1155/2020/8837893.

Jóźwiak, K., Płazińska, A., 2021. Structural insights into ligand—receptor interactions involved in biased agonism of G-protein coupled receptors. Molecules 26 (4), 851. https://doi.org/10.3390/molecules26040851.

Ju, M.S., Lee, P., Kim, H.G., Lee, K.Y., Hur, J., Cho, S.-H., Sung, S.H., Oh, M.S., 2010. Protective effects of standardized *Thuja orientalis* leaves against 6-hydroxydopamine-induced neurotoxicity in SH-SY5Y cells. Toxicol. Vitro 24 (3), 759–765. https://doi.org/10.1016/j.tiv.2009.12.026.

Kalyanasundar, B., Perez, C.I., Arroyo, B., Moreno, M.G., Gutierrez, R., 2020. The appetite suppressant D-norpseudoephedrine (cathine) acts via D1/D2-like dopamine receptors in the nucleus accumbens shell. Front. Neurosci. 14, e572328. https://doi.org/10.3389/fnins.2020.572328.

Kannan, K., Jain, S.K., 2000. Oxidative stress and apoptosis. Pathophysiology 7 (3), 153–163. https://doi.org/10.1016/S0928-4680(00)00053-5.

Kawahata, I., Finkelstein, D.I., Fukunaga, K., 2024. Dopamine D1–D5 receptors in brain nuclei: implications for health and disease. Receptors 3 (2), 155–181. https://doi.org/10.3390/receptors3020009.

Ke, M., Chong, C.-M., Zhu, Q., Zhang, K., Cai, C.-Z., Lu, J.-H., Qin, D., Su, H., 2021. Comprehensive perspectives on experimental models for Parkinson's disease. Aging Dis. 12 (1), 223. https://doi.org/10.14336/AD.2020.0331.

Keane, P., Kurzawa, M., Blain, P., Morris, C., 2011. Mitochondrial Dysfunction in Parkinson's disease, vol 2011. Parkinsons Dis. https://doi.org/10.4061/2011/716871.

Koklesova, L., Liskova, A., Samec, M., Zhai, K., Al-Ishaq, R.K., Bugos, O., Šudomová, M., Biringer, K., Pec, M., Adamkov, M., 2021. Protective effects of flavonoids against mitochondriopathies and associated pathologies: focus on the predictive approach and personalized prevention. Int. J. Mol. Sci. 22 (16), 8649. https://doi.org/10.3390/ijms22168649.

Lamina, S., 2010. Khat (Catha edulis): the herb with officio-legal, socio-cultural and economic uncertainty. S. Afr. J. Sci. 106 (3), 1–4. https://doi.org/10.4102/sajs.v106i3/4.155.

Latchoumycandane, C., Anantharam, V., Jin, H., Kanthasamy, A., Kanthasamy, A., 2011. Dopaminergic neurotoxicant 6-OHDA induces oxidative damage through proteolytic activation of PKCδ in cell culture and animal models of Parkinson's disease. Toxicol. Appl. Pharmacol. 256 (3), 314–323. https://doi.org/10.1016/j.taap.2011.07.021.

Lees, A., 1993. Dopamine agonists in Parkinson's disease: a look at apomorphine. Fund. Clin. Pharmacol. 7 (3-4), 121–128. https://doi.org/10.1111/j.1472-8206.1993.tb00226.x.

Lemos, A., Melo, R., Preto, A.J., Almeida, J.G., Moreira, I.S., Dias Soeiro Cordeiro, M.N., 2018. In silico studies targeting G-protein coupled receptors for drug research against Parkinson's disease. Curr. Neuropharmacol. 16 (6), 786–848. https://doi.org/10.2174/1570159X16666180308161642.

Leong, H.S., Philp, M., Simone, M., Witting, P.K., Fu, S., 2020. Synthetic cathinones induce cell death in dopaminergic SH-SY5Y cells via stimulating mitochondrial dysfunction. Int. J. Mol. Sci. 21 (4), 13–70. https://doi.org/10.3390/ijms21041370.

Liu, Y., Guo, Y., An, S., Kuang, Y., He, X., Ma, H., Li, J., Lv, J., Zhang, N., Jiang, C., 2013. Targeting caspase-3 as dual therapeutic benefits by RNAi facilitating brain-targeted nanoparticles in a rat model of Parkinson's disease. PLoS One 8 (5), e62905. https://doi.org/10.1371/journal.pone.0062905.

Lochner, M., Thompson, A.J., 2016. The muscarinic antagonists scopolamine and atropine are competitive antagonists at 5-HT3 receptors. Neuropharmacol 108, 220–228. https://doi.org/10.1016/j.neuropharm.2016.04.027.

Lopes, F.M., Schröder, R., da Frota Júnior, M.L.C., Zanotto-Filho, A., Müller, C.B., Pires, A.S., Meurer, R.T., Colpo, G.D., Gelain, D.P., Kapczinski, F., 2010. Comparison between proliferative and neuron-like SH-SY5Y cells as an *in vitro* model for Parkinson disease studies. Brain Res. 1337, 85–94. https://doi.org/10.1016/j.brainres.2010.03.102.

Lopez-Suarez, L., Al Awabdh, S., Coumoul, X., Chauvet, C., 2022. The SH-SY5Y human neuroblastoma cell line, a relevant in vitro cell model for investigating neurotoxicology in human: focus on organic pollutants. Neurotoxicology 92, 131–155. https://doi.org/10.1016/j.neuro.2022.07.008.

Luo, Y., Sakamoto, K., 2023. Ethyl pyruvate protects SHSY5Y cells against 6-hydroxydopamine-induced neurotoxicity by upregulating autophagy. PLoS One 18 (2), e0281957. https://doi.org/10.1371/journal.pone.0281957.

Luo, Y., Zhou, S., Takeda, R., Okazaki, K., Sekita, M., Sakamoto, K., 2022. Protective effect of amber extract on human dopaminergic cells against 6-hydroxydopamine-induced neurotoxicity. Molecules 27 (6), 1817. https://doi.org/10.3390/molecules27061817.

Magnavacca, A., Giuliani, C., Roda, G., Piazza, S., Martinelli, G., Pozzoli, C., Maranta, N., Papini, A., Bottoni, M., Casagni, E., 2024. Catha edulis leaves: morphological characterization and anti-inflammatory properties in an in vitro model of gastritis. Plants 13 (11), 1538. https://doi.org/10.3390/plants13111538.

Matcha, R., Saride, G.K., Ranjan, S., 2013. In vitro antiinflammatory and antioxidant activity of leaf extracts of *Datura metal*. Asian J. Pharm. Clin. Res. 6 (4), 146–149.

Mathur, N., Sai, S., Shandily, S., Santoki, K.M., Vadhavana, N.N., Shah, S., Chandra, M., 2024. In Silico Docking: Protocols for Computational Exploration of Molecular Interactions. IntechOpen. https://doi.org/10.5772/intechopen.1005527.

Meng, K., Jia, H., Hou, X., Zhu, Z., Lu, Y., Feng, Y., Feng, J., Xia, Y., Tan, R., Cui, F., 2025. Mitochondrial dysfunction in neurodegenerative diseases: mechanisms and corresponding therapeutic strategies. Biomedicines 13 (2), 327. https://doi.org/10.3390/biomedicines13020327.

Mianda, S.M., Invernizzi, L., van der Watt, M.E., Reader, J., Moyo, P., Birkholtz, L.-M., Maharaj, V.J., 2022. In vitro dual activity of Aloe marlothii roots and its chemical constituents against Plasmodium falciparum asexual and sexual stage parasites. J. Ethnopharmacol. 297, 115551. https://doi.org/10.1016/j.jep.2022.115551.

Miraldi, E., Masti, A., Ferri, S., Comparini, I.B., 2001. Distribution of hyoscyamine and scopolamine in *Datura stramonium*. Fitoterapia 72 (6), 644–648. https://doi.org/10.1016/S0367-326X(01)00291-X.

Mishra, D., 2018. *Datura stramonium* (common name: Jimson weed) medicinal uses, side effects and benefits. World J. Pharm. Res. 7 (12), 1011–1019. https://doi.org/10.20959/wjpr201812-12710.

Mohd Sairazi, N.S., Sirajudeen, K., 2020. Natural products and their bioactive compounds: neuroprotective potentials against neurodegenerative diseases. Evid.-Based Complement. Altern. Med. 2020 (1), e6565396. https://doi.org/10.1155/2020/6565396.

Moon, H.E., Paek, S.H., 2015. Mitochondrial dysfunction in Parkinson's disease. Exp. Neurobiol. 24 (2), 103. https://doi.org/10.5607/en.2015.24.2.103.

Moosavi, M., Farrokhi, M.R., Tafreshi, N., 2018. The effect of curcumin against 6-hydroxydopamine induced cell death and Akt/GSK disruption in human neuroblastoma cells. Physiol. Pharmacol. 22 (3), 163–171. http://ppj.phypha.ir/article-1-1375-en.html.

Mustafa, M., Ahmad, R., Tantry, I.Q., Ahmad, W., Siddiqui, S., Alam, M., Abbas, K., Moinuddin, Hassan, M.I., Habib, S., 2024. Apoptosis: a comprehensive overview of signaling pathways, morphological changes, and physiological significance and therapeutic implications. Cells 13 (22), 1838. https://doi.org/10.3390/cells13221838.

Nataraj, J., Manivasagam, T., Thenmozhi, A.J., Essa, M.M., Khan, M.A., 2016. Antiparkinsonic effect of black tea and its components. In: Essa, M.M., Khan, M.A., Lohano, W.E. (Eds.), Food Parkinson's Dis. Nova Science Publishers, pp. 115–131.

Niemann, B., Rohrbach, S., 2016. Metabolically relevant cell biology–role of intracellular organelles for cardiac metabolism. In: The Scientist's Guide to Cardiac Metabolism, pp. 19–38. https://doi.org/10.1016/B978-0-12-802394-5.00003-0.

Noui, A., Boudiar, T., Boulebd, H., Gali, L., del Mar Contreras, M., Segura-Carretero, A., Nieto, G., Akkal, S., 2022. HPLC–DAD–ESI/MS profiles of bioactive compounds, antioxidant and anticholinesterase activities of *Ephedra alata* subsp. alenda growing in Algeria. Nat. Prod. Res. 36 (22), 5910–5915. https://doi.org/10.1080/14786419.2021.2024184.

Ou, Z., Pan, J., Tang, S., Duan, D., Yu, D., Nong, H., Wang, Z., 2021. Global trends in the incidence, prevalence, and years lived with disability of Parkinson's disease in 204 countries/territories from 1990 to 2019. Front. Public Health 9, 776847. https://doi.org/10.3389/fpubh.2021.776847.

Pallavi Sharma, P.S., Richa Bhardwaj, R.B., Ankita Yadav, A.Y., Sharma, R., 2014. Study of antioxidant activity of Datura stramonium Linn. Res. J. Phytochem. 8 (3), 112–118. =rjphyto.2014.112.118&org=10.

Papadimitriou, M., Hatzidaki, E., Papasotiriou, I., 2019. Linearity comparison of three colorimetric cytotoxicity assays. J. Cancer Ther. 10 (7), 580–590. https://doi.org/10.4236/jct.2019.107047.

Pasban-Aliabadi, H, Esmaeili-Mahani, S, Sheibani, V, Abbasnejad, M, Mehdizadeh, A, Yaghoobi, MM, 2013. Inhibition of 6-hydroxydopamine-induced PC12 cell apoptosis by olive (Olea europaea L.) leaf extract is performed by its main component oleuropein. Rejuvenation Research 16 (2), 134–142. https://doi.org/10.1089/rej.2012.13.

Paz-Ramos, M.I., Cruz, S.L., Violante-Soria, V., 2023. Amphetamine-type stimulants: novel insights into their actions and use patterns. Rev. Invest. Clin. 75 (3), 143–157. https://doi.org/10.24875/ric.23000110.

Radad, K., Moldzio, R., Krewenka, C., Kranner, B., Rausch, W.D., 2023. Pathophysiology of non-motor signs in Parkinsons disease: some recent updating with brief presentation. Explor. Neuroprotective Ther. 3 (1), 24–46. https://doi.org/10.37349/ent.2023.00036.

Ramesh, S., Arachchige, A.S.P.M., 2023. Depletion of dopamine in Parkinson's disease and relevant therapeutic options: a review of the literature. AIMS Neurosci. 10 (3), 200. https://doi.org/10.3934/Neuroscience.2023017.

Rathinam, R., Ghosh, S., Neumann, W.L., Jamesdaniel, S., 2015. Cisplatin-induced apoptosis in auditory, renal, and neuronal cells is associated with nitration and downregulation of LMO4. Cell Death Discov. 1 (1), 1–8. https://doi.org/10.1038/cddiscovery.2015.52.

Roy, A., Khan, A., Ahmad, I., Alghamdi, S., Rajab, B.S., Babalghith, A.O., Alshahrani, M. Y., Islam, S., Islam, M.R., 2022. Flavonoids a bioactive compound from medicinal plants and its therapeutic applications. BioMed Res. Int. 2022 (1), 5445291. https://doi.org/10.1155/2022/5445291.

Roy, S., Pawar, S., Chowdhary, A., 2016. Evaluation of in vitro cytotoxic and antioxidant activity of Datura metel Linn. and Cynodon dactylon Linn. extracts. Pharmacogn. Res. 8 (2), 123. https://doi.org/10.4103/0974-8490.175610.

Sengupta, T., Vinayagam, J., Nagashayana, N., Gowda, B., Jaisankar, P., Mohanakumar, K., 2011. Antiparkinsonian effects of aqueous methanolic extract of Hyoscyamus niger seeds result from its monoamine oxidase inhibitory and hydroxyl radical scavenging potency. Neurochem. Res. 36, 177–186. https://doi.org/10.1007/s11064-010-0289-x.

Senior, T., Botha, M.J., Kennedy, A.R., Calvo-Castro, J., 2020. Understanding the contribution of individual amino acid residues in the binding of psychoactive substances to monoamine transporters. ACS Omega 5 (28), 17223–17231. https://doi.org/10.1021/acsomega.0c01370.

Sharma, M., Dhaliwal, I., Rana, K., Delta, A.K., Kaushik, P., 2021. Phytochemistry, pharmacology, and toxicology of *Datura* species—A review. Antioxidants 10 (8), 1291. https://doi.org/10.3390/antiox10081291.

Shih, Y-T, Chen, I-J, Wu, Y-C, Lo, Y-C, 2011. San-Huang-Xie-Xin-Tang protects against activated microglia-and 6-OHDA-induced toxicity in neuronal SH-SY5Y cells. Evidence-Based Complementary and Alternative Medicine 2011 (1), 429384. https://doi.org/10.1093/ecam/nep025.

Silva, J., Alves, C., Pinteus, S., Mendes, S., Pedrosa, R., 2018. Neuroprotective effects of seaweeds against 6-hydroxidopamine-induced cell death on an *in vitro* human neuroblastoma model. BMC Complement. Altern. Med. 18, 1–10. https://doi.org/10.1186/s12906-018-2103-2.

Smith, M.P., Cass, W.A., 2007. Oxidative stress and dopamine depletion in an intrastriatal 6-hydroxydopamine model of Parkinson's disease. Neuroscience 144 (3), 1057–1066. https://doi.org/10.1016/j.neuroscience.2006.10.004.

Soni, P., Siddiqui, A.A., Dwivedi, J., Soni, V., 2012. Pharmacological properties of *Datura stramonium L.* as a potential medicinal tree: an overview. Asian Pac. J. Trop. Biomed. 2 (12), 1002–1008. https://doi.org/10.1016/S2221-1691(13)60014-3.

Stafford, G.I., Jäger, A.K., van Staden, J., 2005. Activity of traditional South African sedative and potentially CNS-acting plants in the GABA-benzodiazepine receptor assay. J. Ethnopharmacol. 100 (1–2), 210–215. https://doi.org/10.1016/j.jep.2005.04.004.

Sumarac, S., Spencer, K.A., Steiner, L.A., Fearon, C., Haniff, E.A., Kühn, A.A., Hodaie, M., Kalia, S.K., Lozano, A., Fasano, A., 2024. Interrogating basal ganglia circuit function in people with Parkinson's disease and dystonia. eLife 12. https://doi.org/10.7554/eLife.90454. RP90454.

Susin, SA, Lorenzo, HK, Zamzami, N, Marzo, I, Snow, BE, Brothers, GM, Mangion, J, Jacotot, E, Costantini, M, Loeffler, M, Larochette, N, Goodlett, DR, Aebersold, R, Siderovski, DP, Penninger, JM, Kroemer, G, 1999. Molecular characterization of mitochondrial apoptosis-inducing factor. Nature 397 (6718), 441–446. https://doi.org/10.1038/17135.

Suthprasertporn, N., Mingchinda, N., Fukunaga, K., Thangnipon, W., 2020. Neuroprotection of SAK3 on scopolamine-induced cholinergic dysfunction in human neuroblastoma SH-SY5Y cells. Cytotechnology 72, 155–164. https://doi.org/10.1007/s10616-019-00366-7.

Tamuli, R., Mellick, G.D., Schirra, H.J., Feng, Y., 2025. Mode of action of toxin 6-Hydroxydopamine in SH-SY5Y using NMR metabolomics. Molecules 30 (16), 3352. https://doi.org/10.3390/molecules30163352.

Tatton, W.G., Chalmers-Redman, R., Brown, D., Tatton, N., 2003. Apoptosis in Parkinson's disease: signals for neuronal degradation. Ann. Neurol. 53 (S3), S61–S72. https://doi.org/10.1002/ana.10489.

Umarudeen, A.M., Khan, F., Tahir, Y., Modibbo, M.R., 2023. Evaluation of the neurobehavioural toxicity potential of aqueous ethanol extracts of leaf/seed of *Datura metel, Mucuna pruriens*, and T*apinanthus globiferus* growing on Azadirachta indica host tree in mice. Int. J. Biochem. Res. Rev. 32 (8), 13–27. https://doi.org/10.9734/ijbcrr/2023/v32i8831.

Valente, MJ, Bastos, ML, Fernandes, E, Carvalho Fl, 2017. Guedes de Pinho P, Carvalho Mr. Neurotoxicity of β-keto amphetamines: Deathly mechanisms elicited by methylone and mdpv in human dopaminergic SH-SY5Y cells. ACS Chemical Neuroscience 8 (4), 850–859. https://doi.org/10.1021/acschemneuro.6b00421.

Vassilakis, C., Pantidou, A., Psillakis, E., Kalogerakis, N., Mantzavinos, D., 2004. Sonolysis of natural phenolic compounds in aqueous solutions: degradation pathways and biodegradability. Water Res. 38 (13), 3110–3118. https://doi.org/10.1016/j.watres.2004.04.014.

Vélez-Huerta, J., Ramírez-Cabrera, M.A., González-Santiago, O., Favela-Hernández, J.M. d.J., Arredondo-Espinoza, E.U., Balderas-Rentería, I., 2022. Neuroprotective activity of *Datura inoxia* and *Turnera diffusa* extracts in an *in vitro* model of neurotoxicity. Pharmacogn. Mag. 18 (78). https://doi.org/10.4103/pm.pm_543_21.

Vichai, V., Kirtikara, K., 2006. Sulforhodamine B colorimetric assay for cytotoxicity screening. Nat. Protoc. 1 (3), 1112–1116. https://doi.org/10.1038/nprot.2006.179.

Vinokur, Y., 2008. Hydrophilic and lipophilic antioxidant capacity and content of phenolic compounds in fresh khat leaves (*Catha edulis* Forsk.). Ethnobot. Leaflets. 2008 (1), 73. https://opensiuc.lib.siu.edu/ebl/vol2008/iss1/73.

Wabe, N.T., 2011. Chemistry, pharmacology, and toxicology of khat (*Catha edulis* forsk): a review. Addict. Health 3 (3–4), 137.

Wang, H., Chen, Y., Wang, L., Liu, Q., Yang, S., Wang, C., 2023. Advancing herbal medicine: enhancing product quality and safety through robust quality control practices. Front. Pharmacol. 14, 1265178. https://doi.org/10.3389/fphar.2023.1265178.

Wang, S., Che, T., Levit, A., Shoichet, B.K., Wacker, D., Roth, B.L., 2018. Structure of the D2 dopamine receptor bound to the atypical antipsychotic drug risperidone. Nature 555 (7695), 269–273. https://doi.org/10.1038/nature25758.

Wei, L, Ding, L, Mo M-s, Lei, M, Zhang, L, Chen, K, Xu, P, 2015. Wnt3a protects SH-SY5Y cells against 6-hydroxydopamine toxicity by restoration of mitochondria function. Translational Neurodegeneration 4 (11), 1–8. https://doi.org/10.1186/s40035-015-0033-1.

White, J.B., Beckford, J., Yadegarynia, S., Ngo, N., Lialiutska, T., d'Alarcao, M., 2012. Some natural flavonoids are competitive inhibitors of caspase-1, -3, and-7 despite their cellular toxicity. Food Chem. 131 (4), 1453–1459. https://doi.org/10.1016/j.foodchem.2011.10.026.

Xie X, H.-r., Hu, L.-s., Li, G.-y., 2010. SH-SY5Y human neuroblastoma cell line: in vitrocell model of dopaminergic neurons in Parkinson's disease. Chin. Med. J. 123 (8), 1086–1092. https://doi.org/10.3760/cma.j.issn.0366-6999.2010.08.021.

Yadav, B., Singla, A., Srivastava, N., Gupta, P., 2021. Pharmacognostic and phytochemical screening of *Datura stramonium* by TLC and GC-MS: a forensic approach. Biomed. Pharmacol. J. 14 (4), 2221–2226. https://doi.org/10.13005/bpj/2320.

Ye, S., Hu, J., Liu, Z., Liang, M., 2021. Progress and research trends on *Catha edulis* (Vahl) Endl. (*Catha edulis*): a review and bibliometric analysis. Front. Pharmacol. 12, e705376. https://doi.org/10.3389/fphar.2021.705376.

Zhou, X., 2020. Molecular Toxicological Mechanisms of New Psychoactive Substances" in Vitro. [University_of_Basel].

Zhuang, Y., Krumm, B., Zhang, H., Zhou, X.E., Wang, Y., Huang, X.-P., Liu, Y., Cheng, X., Jiang, Y., Jiang, H., 2021. Mechanism of dopamine binding and allosteric modulation of the human D1 dopamine receptor. Cell Res. 31 (5), 593–596. https://doi.org/10.1038/s41422-021-00482-0.

Zuo, L., Motherwell, M.S., 2013. The impact of reactive oxygen species and genetic mitochondrial mutations in Parkinson's disease. Gene 532 (1), 18–23. https://doi.org/10.1016/j.gene.2013.07.085.